ILC Staging and Running Scenarios

ILC Parameters Joint Working Group

T. Barklow, J. Brau, K. Fujii, J. Gao, J. List, N. Walker, K. Yokoya

Abstract

The preferred scenario for realizing the ILC involves construction of the full 500 GeV machine from the start, as documented by the design in the ILC Technical Design Report. In planning for the ILC hosted by and based in Japan it has been suggested that a staged energy implementation might be necessary, starting at a centre-of-mass energy of at least 250 GeV before upgrading eventually to 500 GeV. The later 1 TeV upgrade is also preserved. This report considers the tradeoffs for various staging scenarios, including a realistic estimate of the real time accumulation of integrated luminosity based on ramp-up and upgrade processes. The report concentrates on the physics reach up to $\sim$ 500 GeV. Various physics outcomes are presented for each of the scenarios. While the majority of the report addresses the 250 GeV - 500 GeV staging plan, the scientific advantages of starting operations at 350 GeV, and extending the 500 GeV machine to $\sim$ 550 GeV are discussed. In addition to the certain precision physics that is the main focus of this study, there are existing scientific motivations that indicate the real possibility for discoveries of new particles in the upcoming operations of the LHC or the early operation of the ILC. Follow-up studies of such discoveries could alter the plan for the centre-of-mass collision energy of the ILC and expand even more the scientific impact of the ILC physics program.

1 Introduction

The ILC requirements document "Parameters for the Linear Collider" [1] describes the basic requirements for a 500 GeV centre-of-mass machine with the possibility of extending the energy up to 1 TeV. The ILC design given in the Technical Design Report (TDR) realizes this machine. This implementation (constructing a full 500 GeV collider from the start) remains the preferred approach.

Following the discovery of the Higgs boson at the LHC, the Japan Association of High Energy Physicists (JAHEP) recommended that the ILC physics studies "shall start with a precision study of the Higgs boson and then evolve into studies of the top quark, dark matter particles, and the Higgs self-couplings, by upgrading the accelerator. A more specific scenario is as follows:

- A Higgs factory with a centre-of-mass energy of approximately 250 GeV shall be constructed as the first phase.
- The machine shall be upgraded in stages up to a centre-of-mass energy of ∼500 GeV which is the baseline energy of the overall project.
- Technical extendibility to a 1 TeV region shall be preserved."

A multiple staged energy implementation, while technically feasible, will require several stop-start cycles with associated complications. The JAHEP statement may be interpreted to mean a project with a first stage of 250 GeV. A pause in installation would then ensue to allow for a period of commissioning (∼1 year) and physics operation of approximately 4 years after which time a single shutdown of ∼18 months would be used to complete the project to 500 GeV.

This is consistent with the TDR physics goal of 250 fb^{-1} of integrated luminosity at 250 GeV using the nominal TDR peak luminosity of 7.5×10^{33} $\text{cm}^{-2}\text{s}^{-1}$ and assuming a yearly luminosity progression of 10%, 30%, and 60% of peak as proposed in the requirements document as well as 75% efficiency for eight (8) months per year (or $\sim 1.6 \times 10^7$ seconds/year).

However, this represents a significantly different construction scenario from that described in the TDR with impact on the overall schedule and the associated sub-system planning. The TDR specifies construction at the start of the full 500 GeV project. While this remains the preferred approach to realizing the ILC, the impacts of this different construction scenario were addressed by Dugan, Harrison, List and Walker in their note [2] "Implications of an Energy-Phased approach to the realization of the ILC." The note was intended to outline for planning purposes, the major changes to the TDR arising from this phased energy approach.

Following this initial consideration given to the machine construction issues, a study has been conducted to understand the physics implications of the staging choices. An ILC Parameters Joint Working Group was created by the LCC Directorate with the following charge:

> The ILC parameter working group reports to the LCC Directorate. It consists of members from both the ILC accelerator and the physics & detector groups where each team selects a co-convener for this working group.
>
> This working group prepares information on ILC machine parameters and staging scenarios as well as potential upgrade paths in a form readily usable by the LCC. In doing so, the WG will take into account technical machine constraints and physics and detector needs regarding the fundamental ILC machine parameters such as energy, luminosity, crossing angles, etc.
>
> The first task for the working group is to prepare multiple scenarios for staging up to about 500 GeV. The report should contain the pros and cons of each scenario as well as luminosities needed at each energy to produce corresponding physics results.

In order to quantify the impact of various options of running on the physics output, and particularly on its evolution with time, ten operating scenarios were initially considered. Operating scenarios must be distinguished from the staging scenarios. Staging refers to the installed energy capability of the collider. Operating specifies the collision energy. In other words, operations may be conducted at a lower energy than the full capability of the collider once a staging upgrade has been implemented. The ten initial scenarios were reduced to four which are described in the remainder of this document.

It must be emphasized that one of the very valuable features of the ILC is its energy flexibility. Discoveries made at the LHC or in the early phases of the ILC will impact the choice of operating energies; once the collider has achieved a particular maximum energy reach, it can operate at lower energies as the physics requirements dictate. Such potential discoveries cannot be specified with certainty today, but would greatly expand the scientific impact of the ILC and broaden its follow-on program.

The principal physics motivations for operations in the 250-500 GeV range are a high-precision characterisation of the recently discovered Higgs boson and high-precision determination of the properties of the top quark. Together with precision measurements of the W and Z boson masses and couplings, they provide powerful tools for discovering beyond the Standard Model physics. The precision part of the ILC program will be complemented by searches for direct production of new particles, in particular for Dark Matter candidates. Once new particles in the kinematic reach of the ILC have been discovered, either at the LHC or at the ILC itself, precision measurements of their masses and chiral couplings will allow unveiling of the type of the underlying extension of the Standard Model and its fundamental parameters. More details on the physics program of the ILC can be found in [3].

Before comparing different staging and operation scenarios of the ILC, we briefly summarize the interplay of the various center-of-mass energies for the main topics of the ILC physics program:

- Higgs precision measurements: In e^+e^- collisions, Higgs bosons can be produced either via their coupling to the Z boson ("Higgsstrahlung"), or via their coupling to

the W boson ("WW fusion"). At $\sqrt{s} = 250\,\text{GeV}$, the production occurs dominantly through Higgsstrahlung. This is very beneficial for the fully model-independent recoil method for measuring the total ZH cross-section and the Higgs mass, but on the other hand there is limited sensitivity to the Higgs-W coupling. For $350\,\text{GeV} \lesssim \sqrt{s} \lesssim 550\,\text{GeV}$, these two production modes are of similar size, which yields a balanced sensitivity to both the Higgs-W and the Higgs-Z couplings. Probing the top-Yukawa coupling from associated production of $t\bar{t}H$ requires at least $\sqrt{s} \gtrsim 500\,\text{GeV}$. Due to these three production processes, Higgs physics exhibits the most complex interplay between different center-of-mass energies, which we will discuss in more detail in the following sections.

- Top quark precision measurements: At the ILC with $\sqrt{s} \gtrsim 350\,\text{GeV}$, top quark pairs will be produced for the very first time in e^+e^- collisions. A variation of $\sqrt{s}$ near 350 GeV will give a quantitatively and qualitatively unique measurement of the top quark mass. However, deviations of the electro-weak couplings of the top quark from their Standard Model values, which are predicted by many extensions of the Standard Model, can only be detected at higher $\sqrt{s} \gtrsim 450\,\text{GeV}$, since near threshold they are buried beneath the remnant of the strong $t\bar{t}$ 1S resonance.

- Couplings and masses of the W and Z bosons: A powerful probe for physics beyond the Standard Model are triple and quartic gauge couplings. While they can in principle be probed at any center-of-mass energy which allows di-boson production, the sensitivity rises strongly with $\sqrt{s}$. For instance in the case of charged triple gauge couplings, the ILC with $\sqrt{s} = 500\,\text{GeV}$ will increase the sensitivity by two orders of magnitude with respect to LEP2. The W boson mass measurement can reach the few MeV regime either from a scan of the production threshold near $\sqrt{s} = 161\,\text{GeV}$, or from kinematic reconstruction at $\sqrt{s} = 500\,\text{GeV}$. Concerning the Z boson, operation of the ILC near $\sqrt{s} = 90\,\text{GeV}$ with polarised beams could be the only possibility to resolve the existing tension between the left-right asymmetry measured at SLD and the forward-backward asymmetry from LEP. Also an improvement of the Z mass measurement beyond LEP is conceivable.

- Production of new particles, including Dark Matter: The reach for the pair production of new particles and thus the possibility for direct discoveries obviously increases with center-of-mass energy and covers almost $M < \sqrt{s}/2$. In new physics models where the production cross-sections are not given by Standard Model couplings (as e.g. in SUSY), higher center-of-mass energy allows the probing of smaller couplings, thus higher scales of new physics.

These physics motivations have driven the design of the staging scenarios.

The TDR presented a baseline machine with $\sqrt{s} = 500\,\text{GeV}$. Figure 1 shows the time evolution of the statistical precisions on the Higgs' couplings achievable with this baseline machine operating at $\sqrt{s}$=500 GeV as a function of real time until a total integrated luminosity of $2.5\,\text{ab}^{-1}$ is reached. This time evolution serves as a reference for comparison with different staging scenarios.

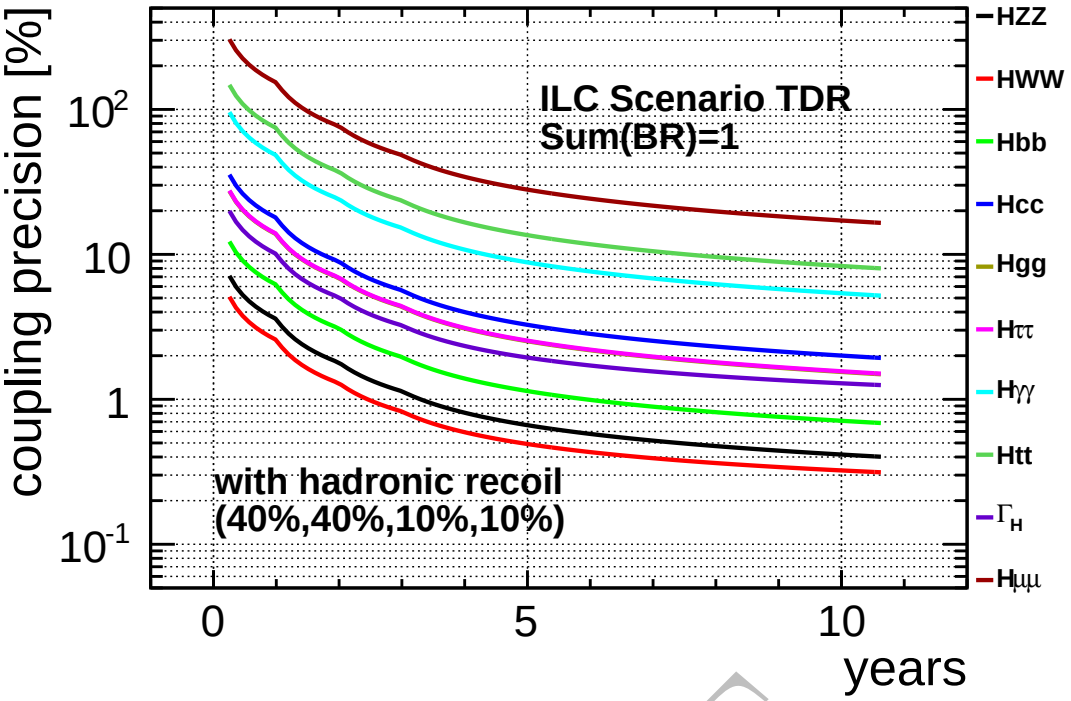

Figure 1: Statistical uncertainty of Higgs couplings in the TDR baseline ILC operating at $\sqrt{s} = 500\,\text{GeV}$ as a function of real time, including ramp-up as discussed in section 3, and assuming the luminosity sharing between the beam helicity configurations discussed in section 2.1.

The remainder of this report is structured as follows: We start in section 2 by introducing different scenarios for operating the ILC starting with a staged machine at $\sqrt{s} = 250\,\text{GeV}$. In section 3, the derivation of the real time need of these scenarios is explained. Section 4 gives examples for the time evolution of different physics observables in selected running scenarios. In section 5 we lay out the advantages of starting ILC operations at 350 GeV, if possible. Section 6 discusses the top Yukawa coupling reach at the maximum energy of $\sqrt{s} \sim 500$ GeV. Finally we comment on the luminosity needs at other centre-of-mass energies in section 7, including both operation below $\sqrt{s} = 200\,\text{GeV}$ and at $\sqrt{s} = 1\,\text{TeV}$, before concluding the report in section 8.

2 Running Scenarios starting at $\sqrt{s} = 250\,\text{GeV}$

2.1 Integrated luminosities and polarisation splitting

The total integrated luminosities collected at various center-of-mass energies will determine the ultimate physics reach of the ILC. It is not clear now what the best combination of dataset sizes will be following the upcoming LHC running as well as early ILC operation. We present a few scenarios which could be chosen based on what is known of

the physics at that time. For center-of-mass energies of $\sqrt{s} = 250, 350$ and $500\,\text{GeV}$, we propose the examples presented in earlier sections and listed in table 1 for studying this issue. In particular, the scenarios "C-250" and "C-500" serve to illustrate different balancing between $\sqrt{s} = 250$, 350, and 500 GeV. It must be kept in mind that other operating energies may be required based on the physics results from the LHC or early ILC.

	$\int \mathcal{L}dt$ [fb^{-1}]			
$\sqrt{s}$	A	B	C-250	C-500
250 GeV	2000	2000	2000	500
350 GeV	200	200	200	200
500 GeV	3000	3000	3500	5500

Table 1: Proposed total target integrated luminosities for $\sqrt{s} = 250, 350, 500\,\text{GeV}$.

The ultimate physics reach further depends on the assumed beam polarisations. Concerning the absolute values, the highest achievable degree of polarisation is desirable, in particular for the positron beam. We assume here the TDR values of $|P(e^-)| = 80\%$ and $|P(e^+)| = 30\%$. The option of upgrading to $|P(e^+)| = 60\%$ would enhance the physics potential of the machine, while the absence of positron polarisation would reduce it. The size of the impact depends strongly on the individual physics observables and is beyond the scope of this report, but should be quantified in the near future.

Independent of the absolute values of the beam polarisations, the choice of their signs, i.e. running with predominantly left- or right-handed electrons / positrons is important for the physics program. Due to conservation of angular momentum, the s-channel exchange of Z bosons or photons is only possible for opposite-sign chirality, i.e. $e^-_L e^+_R$ or $e^-_R e^+_L$. Among these, the chiral couplings of the Z boson prefer the former combination. Within the Standard Model (SM), only the t-channel exchange of a Z boson or photon is allowed for like-sign helicities, i.e. $e^-_L e^+_L$ and $e^-_R e^+_R$. Beyond the SM, Majorana particles, for instance neutralinos in supersymmetric extensions, could be exchanged in the t-channel, allowing like-sign helicities as in selectron productions. Only the combination $e^-_L e^+_R$ contributes to t-channel exchange of a W boson or a electron-neutrino. Thus W pair production, which is an important background for many signatures, can be reduced by orders of magnitude by choosing the opposite beam helicities.

	fraction with $\text{sgn}(P(e^-), P(e^+)) =$			
	(-,+)	(+,-)	(-,-)	(+,+)
$\sqrt{s}$	[%]	[%]	[%]	[%]
250 GeV	67.5	22.5	5	5
350 GeV	67.5	22.5	5	5
500 GeV	40	40	10	10

Table 2: Relative sharing between beam helicity configurations proposed for the various center-of-mass energies.

Therefore we propose the sharing between the four possible sign combinations listed in table 2. It should be noted that one profits from the cancellation of experimental systematic uncertainties between these samples only if they are accumulated while flipping the beam helicities in a randomized way on bunch train time-scales. The average flipping frequencies are thereby adjusted to give the helicity fractions listed in table 2.

At $\sqrt{s} = 250$ and 350 GeV, it is expected that the main interest will be on Standard Model processes. Thus 90% of the data is collected in the unlike-sign combinations, preferring left-handed electrons over right-handed. Only a small fraction (10%) of the like-sign configurations is planned to control systematics.

	integrated luminosity with $\mathrm{sgn}(P(e^-), P(e^+)) =$			
	(-,+)	(+,-)	(-,-)	(+,+)
$\sqrt{s}$	[fb^{-1}]	[fb^{-1}]	[fb^{-1}]	[fb^{-1}]
250 GeV	340	110	25	25
350 GeV	135	45	10	10
500 GeV	2200	2200	550	550

Table 3: Integrated luminosities per beam helicity configuration resulting from the fractions in table 2 in scenario C-500.

At higher $\sqrt{s}$, the picture changes because new physics is more likely to appear. For example Dark Matter searches with an effective field theory approach could profit significantly from like-sign data-taking depending on the Lorentz structure of its couplings; also the determination of the chiral properties of new particles requires a more balanced sharing between beam helicity configurations. Indirect searches, e.g. via the electroweak couplings of the top quark, prefer right-handed electrons over left-handed ones. Thus, a splitting of (40%,40%,10%,10%) is proposed here. On the other hand, Higgs production via WW fusion exists only for left-handed electrons and right-handed positrons. Figure 2 shows the same time evolution of precisions as figure 1, but with a splitting of (67.5%,22.5%,5%,5%). The largest improvement occurs as expected for g_{HWW}, which after 5 years reaches a precision of $\sim 0.4\%$, to be compared to $\sim 0.5\%$ with (40%,40%,10%,10%) (c.f. fig 1). We conclude that this improvement does not outweigh the expected loss of sensitivity in other physics, e.g. Dark Matter searches or measurement of the top quark couplings.

Table 3 shows an example case of the resulting integrated luminosities per center-of-mass energy and helicity configuration for the scenario C-500.

It must be stressed once more that a key asset of the ILC is its flexibility. For all center-of-mass energies, further discoveries at the LHC or the results of the first ILC runs could lead to modifications of the ideal sharing between helicity fractions. Such changes in the run plan can easily be accommodated based on future physics results.

2.2 Operation Scenarios

Section 2.1 presents total integrated luminosities which can be collected at different stages of the machine in different periods of time, leading to what we refer to as "running

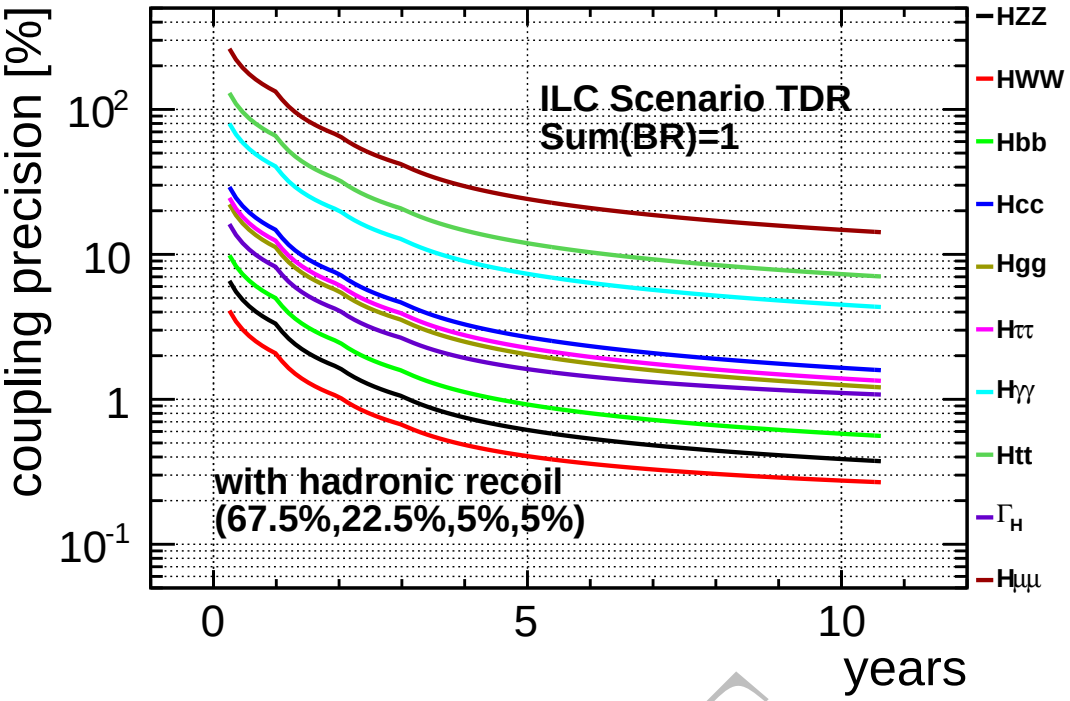

Figure 2: Statistical uncertainty of Higgs couplings in the TDR baseline ILC operating at $\sqrt{s} = 500\,\text{GeV}$ as a function of real time, including ramp-up as discussed in section 3, with a luminosity splitting between beam helicities of (67.5%,22.5%,5%,5%).

scenarios". In this section, we propose a few examples of such running scenarios to be evaluated from the physics perspective, all under the assumption of starting a staged machine at $\sqrt{s} = 250\,\text{GeV}$. We concentrate on two main parameters to vary:

- The integrated luminosity to be collected at $\sqrt{s} = 250\,\text{GeV}$ with an initial staged 250 GeV machine. We will consider 3 cases in the tables below: A) $250\,\text{fb}^{-1}$, B) $500\,\text{fb}^{-1}$, C) $100\,\text{fb}^{-1}$, which corresponds to A) 4.1, B) 6.4, C) 2.8 years of running of the initial 250 GeV staged machine before upgrading it to 500 GeV, including ramp-up.

- The final accumulation of integrated luminosity per energy. In order to limit the number of cases, we only study this variation for the case of scenario C by varying the operation energy for the second half of running time after the luminosity upgrade.

In this we apply the following guidelines/restrictions:

- All scenarios are limited to about equal total operation times near 25 years, before a possible 1 TeV upgrade or other running options.

- All scenarios assume that an integrated luminosity of at least $200\,\text{fb}^{-1}$ will be collected at the top threshold near $\sqrt{s} = 350\,\text{GeV}$. Current studies [4] indicate that the

top mass measurement from a scan of the production threshold becomes theoretically limited for $100\,\text{fb}^{-1}$. In order to allow for data taking with other polarisations, collection of control samples and further improvements of the theoretical calculations we assume here a minimum of $200\,\text{fb}^{-1}$. We assume that this will be done with the 500 GeV machine operated at a reduced gradient, after an initial exploration of the physics landscape at $\sqrt{s} = 500\,\text{GeV}$ and with a well run-in machine.

- At each $\sqrt{s}$, the total integrated luminosities given below should be understood to be split up between the four possible beam helicity configurations as specified in section 2.1.

- In order to give a complete picture of the potential of the ILC, we include a luminosity upgrade and the possibility to provide collisions at more than 5 Hz, when surplus RF and cryogenic power allows.

- The exact details of the very long term program will depend on future developments at early stages of the ILC, at the LHC and possibly other scientific results. Thus we do not speculate here about the possible variations beyond a ~ 25 year program, in particular the upgrade to $\sqrt{s} = 1\,\text{TeV}$. However we note that many measurements of the 500 GeV program could be done even better at $\sqrt{s} = 1\,\text{TeV}$. Thus a realisation of the 1-TeV-upgrade could replace part of the required luminosity at $\sqrt{s} = 500\,\text{GeV}$.

- Further discoveries, in particular also at the inital run of ILC-500, will change the details and might add the necessity to run at additional intermediate energies, either for scanning production thresholds of new particles, or for disentangling several states close by in mass (eg. in SUSY measure the $\tilde{\tau}$ mixing angle in $\tilde{\tau}_1\tilde{\tau}_2$ mixed production below the $\tilde{\tau}_2\tilde{\tau}_2$ pair production threshold).

- We do not list here physics running at the Z-pole or at the WW-threshold. However we note that their physics program should be done at some point, where the timing will depend on the outcome of an inital running at $\sqrt{s} = 500\,\text{GeV}$.

- Runtime on the Z-pole for calibration is also not included. This may be needed annually for detector calibration (e.g. of the momentum scale of the tracking detectors). *Here, more precise specifications from the experiments are needed in order to assess the amount of data needed for reaching which level of calibration precision.*

- The details about the time lines for these scenarios including ramp-up and upgrade-installation times will be presented in section 3.

Table 4 shows the integrated luminosities and real time required for each stage of the four running scenarios presented here. The time estimates include ramp-up efficiencies and installation times for upgrades.

The motivations for each of these scenarios are as follows:

- Scenario A assumes that the canonical amount of $250\,\text{fb}^{-1}$ at $\sqrt{s} = 250\,\text{GeV}$ is collected in the very first run of the ILC before upgrading to the top baseline energy.

	Stage	250	500			500 LumiUP			
Scenario	$\sqrt{s}$ [GeV]	250	500	350	250	500	250	350	500
A	$\int \mathcal{L}dt$ [fb^{-1}]	250	1000	200	750	2000	1000	-	-
	time [years]	4.1	4.9	1.3	4.2	4.9	3.1	-	-
B	$\int \mathcal{L}dt$ [fb^{-1}]	500	1000	200	500	2000	1000	-	-
	time [years]	6.2	4.9	1.3	3.1	4.9	3.1	-	-
C-250	$\int \mathcal{L}dt$ [fb^{-1}]	100	1000	200	400	2500	1500	-	-
	time [years]	2.8	5.5	1.3	2.7	5.8	4.2	-	-
C-500	$\int \mathcal{L}dt$ [fb^{-1}]	100	1000	200	400	2500	-	-	2000
	time [years]	2.8	5.5	1.3	2.7	5.8	-	-	3.5

Table 4: Final integrated luminosities and real time (calendar years) required for each stage of the running scenarios, including ramp up and installation times for upgrades. Not included: calibration and physics runs at Z pole and WW-threshold, scanning of new physics thresholds.

With the current estimates on the ramp-up of luminosity (c.f. section 3), this scenario allows a full running-in of the machine with one year of operation at the design parameters.

- Scenario B serves to illustrate the impact of prolonging the first stage until twice the amount of data is collected at $\sqrt{s} = 250\,\text{GeV}$ before upgrading to the top baseline energy. It focusses on maximizing the early precision on g_{HZZ} and the Higgs recoil mass. For other measurements, results will be delayed.

- The scenarios C-X reduce the duration of the first run at $\sqrt{s} = 250\,\text{GeV}$ to just about the time needed to produce the remaining cryomodules for upgrading to the top baseline energy. As a consequence, the machine is not fully run-in before upgrading to the top baseline energy. On the other hand, this scenario gives the earliest access to important key observables: g_{HWW} (from $\sqrt{s} \geq 350\,\text{GeV}$), g_{Htt} (from $\sqrt{s} \geq 500\,\text{GeV}$), electroweak top couplings(from $\sqrt{s} \geq 450\,\text{GeV}$) and an early increase of sensitivity for triple gauge couplings and direct searches, e.g. for Dark Matter.

  For the long-term program, two C-X variations are considered:

  - Scenario C-250 features a third run 250 GeV after the luminosity upgrade, resulting in 4 times the instantaneous luminosity of the initial 250 GeV run. This would be an option if it turns out that e.g. the Higgs mass measurement precision is not sufficient and a high-statistics version of the recoil mass measurement is required (c.f. section 4.2).
  - Scenario C-500 instead invests all running time after the luminosity upgrade into operation at $\sqrt{s} = 500\,\text{GeV}$.

Table 5 summarizes the run times of the scenarios defined in table 4. The comparison of scenarios A, B and C-250 shows that longer initial running at a staged 250 GeV machine leads to an overall longer time in order to accumulate the same final integrated luminosity.

This is expected since a staged 250 GeV machine provides significantly lower instantaneous luminosity than the 500 GeV baseline machine operated at $\sqrt{s} = 250$ GeV (5 Hz and 10 Hz collisions respectively). The same is true if part of the 250 GeV data-taking can be postponed to the luminosity upgrade phase as assumed in scenarios C-X. In particular C-250 is shorter than A and B but still delivers 500 fb^{-1} more than these two scenarios at 500 GeV.

	total run time *before*		
	500 GeV	Lumi upgrade	TeV upgrade
Scenario	[years]	[years]	[years]
A	4.1	16.0	25.5
B	6.2	17.1	26.6
C-250	2.8	13.8	25.3
C-500	2.8	13.8	24.6

Table 5: Cumulative running times for the four scenarios, including ramp-up and installation of upgrades. Not included: calibration and physics runs at Z pole and WW-threshold or scanning of new physics thresholds.

3 Timelines of the running scenarios

The timelines for integrated luminosity have been estimated and are shown in the plots below under the following assumptions:

Basic assumptions

- All plots are presented in calendar years.
- A full calendar year is assumed to represent eight months running at an efficiency of 75% (the RDR assumption). This corresponds approximately to $Y = 1.6 \times 10^7$ seconds of integrated running. (This is significantly higher than a Snowmass year of 10^7 seconds.)
- t = 0 (start of Year 1) is the start of running for physics. Year 0 (-1 $\leq$ t $<$ 0), directly after construction, is assumed to be for machine commissioning only (not shown in the plots).
- If the peak instantaneous luminosity is L, then the nominal integrated luminosity for a fully-operational calendar year is $L_{int} = L \times Y$. For any given calendar year during a period of ramp-up, the integrated luminosity for that year is $f \times L_{int}$, where f is the ramp fraction associated with that year ($f \leq 1$).

Ramp-up assumptions

- A ramp-up of luminosity performance is in general assumed after: (a) initial construction and after 'year 0' commissioning; (b) after a downtime for an accelerator upgrade (energy to 500 GeV or luminosity); (c) a change in operational mode which may require some learning curve (e.g. going to 10-Hz collisions).
- A ramp is defined as a set of ramp factors f, one factor for each consecutive integral calendar year at the beginning of a specific run.
- For the initial physics run after construction and year 0 commissioning, the RDR ramp of 10%, 30%, 60% and 100% over the first four calendar years is always assumed (all scenarios).
- In general, the ramp after the shutdowns for installation of the remaining linacs (500 GeV machine) or luminosity upgrade is assumed slightly shorter (10%, 50%, 100%) with no year 0.
- Going down in centre of mass energy from 500 GeV to 350 GeV is assumed to have no ramp associated with it, since there is no modification (shutdown) to the machine.
- Going to 10-Hz operation at 50% gradient does assume a ramp however (25%, 75%, 100%), since 10-Hz affects the entire machine including the damping rings and sources etc.

Shutdowns

- Two major 18 month shutdowns are assumed for (a) installation of the remaining linac for the 500 GeV machine, and (b) the luminosity upgrade.
- In both cases, the down-times may be on the optimistic side, but would appear to be roughly consistent with the TDR construction installation rates, assuming that the same level of manpower is available, and that all the necessary components for installation are (mostly) available at the time the shutdown starts.
- The first shutdown is to install the remainder of the main linacs to increase the energy capacity from the initial phase $\sqrt{s} = 250\,\text{GeV}$ to $\sqrt{s} = 500\,\text{GeV}$. This includes removal of the temporary transport lines in the main linac, and subsequent installation of cryomodules, klystrons, modulators, LLRF and associated infrastructure (and possibly cryoplants).
- The second shutdown is for the TDR luminosity upgrade, where the number of bunches per pulse is increased from 1310 to 2620. This requires the installation of an additional 50% of klystrons and modulators, as well as the possible installation of a second positron damping ring. It is assumed that linac and damping ring installation occur in parallel and do not interfere with each other.

	E_{CM}	$\int$Ldt	L_{peak}	Ramp				T	T_{acc}	Comment
				1	2	3	4			
Physics run	250	250	0.75	10	30	60	100	4.1	4.1	TDR nominal operation at 5Hz
Shutdown								1.5	5.6	Upgrade to full 500 GeV machine
Physics run	500	1000	1.8	10	50	100	100	4.9	10.5	TDR nominal operation at 5Hz
Physics run	350	200	1.	100	100	100	100	1.3	11.8	TDR nominal operation at 5Hz
Physics run	250	750	1.5	25	75	100	100	4.2	16.	Operation at 10 Hz
Shutdown								1.5	17.5	Luminosity upgrade
Physics run	500	2000	3.6	10	50	100	100	4.9	22.4	TDR lumi–up at 5Hz
Physics run	250	1000	3.	25	75	100	100	3.1	25.5	TDR lumi–up at 10Hz

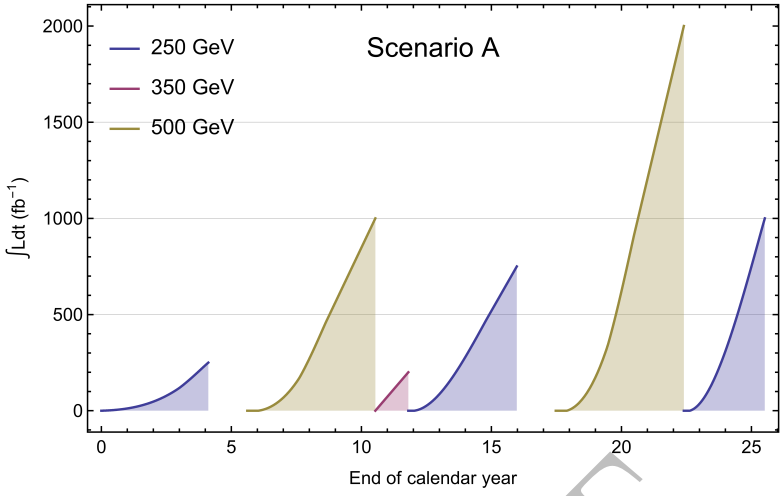

Figure 3: Accumulation of integrated luminosity versus real time for scenario A

Scenarios Each of the staging scenarios (A, B, C-250 and C-500) are represented in Figures 3 through 6. Each figure provides a graph of integrated luminosity versus calendar time at the respective centre-of-mass energies (colour coded), while the associated table provides a summary of the scenario, including the time T for each run segment and the total integrated time T_{acc} (both in calendar years). The Ramp gives the assumed ramp fractions f for the first four years of running for each segment (in percent).

4 Time Development of Physics Results

In this section we present some examples of how important physics results evolve in time for the four scenarios presented above. All plots in this section are preliminary since not all analyses involved have been finished yet, so that some measurements are extrapolated, e.g. from other center-of-mass energies.

4.1 Higgs coupings to fermions and gauge bosons

Figures 7 and 8 show the current snapshot of available Higgs studies interpreted in a fully model-independent global fit. They are in particular preliminary since some of the analyses at $\sqrt{s} = 350\,\text{GeV}$ are not yet finished. A key question is how well the HZZ coupling can be extracted at $\sqrt{s} > 250\,\text{GeV}$.

	E_{CM}	$\int$Ldt	L_{peak}	Ramp				T	T_{acc}	Comment
				1	2	3	4			
Physics run	250	500	0.75	10	30	60	100	6.2	6.2	TDR nominal operation at 5Hz
Shutdown								1.5	7.7	Upgrade to full 500 GeV machine
Physics run	500	1000	1.8	10	50	100	100	4.9	12.7	TDR nominal operation at 5Hz
Physics run	350	200	1.	100	100	100	100	1.3	13.9	TDR nominal operation at 5Hz
Physics run	250	500	1.5	25	75	100	100	3.1	17.	Operation at 10 Hz
Shutdown								1.5	18.5	ScenarioComment
Physics run	500	2000	3.6	10	50	100	100	4.9	23.5	TDR lumi-up at 5Hz
Physics run	250	1000	3.	25	75	100	100	3.1	26.6	TDR lumi-up at 10Hz

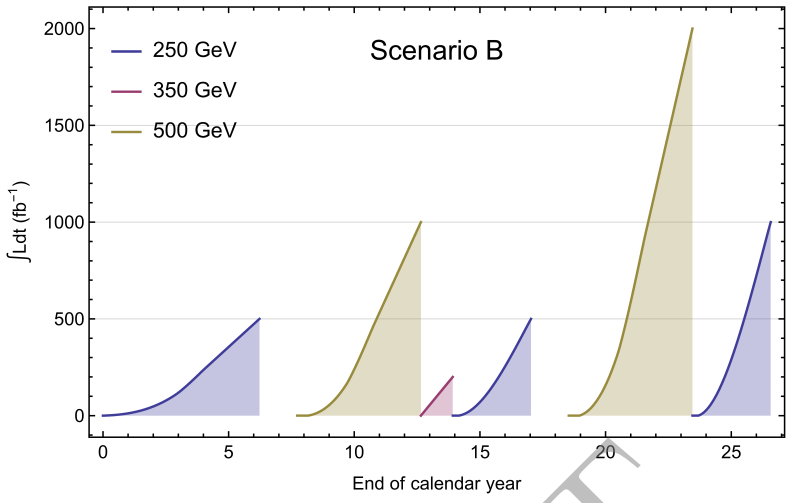

Figure 4: Accumulation of integrated luminosity versus real time for scenario B

	E_{CM}	$\int$Ldt	L_{peak}	Ramp				T	T_{acc}	Comment
				1	2	3	4			
Physics run	250	100	0.75	10	30	60	100	2.8	2.8	TDR nominal operation at 5Hz
Shutdown								1.5	4.3	Upgrade to full 500 GeV machine
Physics run	500	1000	1.8	10	30	60	100	5.5	9.8	TDR nominal operation at 5Hz
Physics run	350	200	1.	100	100	100	100	1.3	11.1	TDR nominal operation at 5Hz
Physics run	250	400	1.5	25	75	100	100	2.7	13.8	Operation at 10 Hz
Shutdown								1.5	15.3	Luminosity upgrade
Physics run	500	2500	3.6	10	50	100	100	5.8	21.1	TDR lumi-up at 5Hz
Physics run	250	1500	3.	25	75	100	100	4.2	25.3	TDR lumi-up at 10Hz

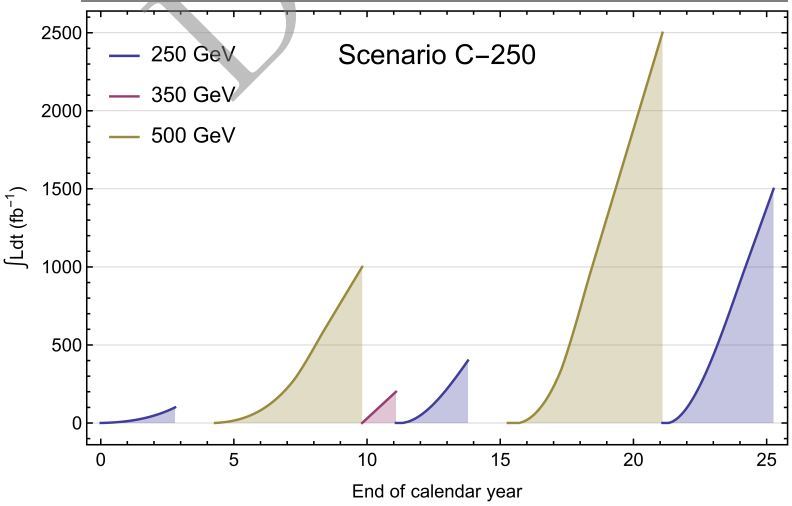

Figure 5: Accumulation of integrated luminosity versus real time for scenario C-250

	E_{CM}	$\int$Ldt	L_{peak}	Ramp				T	T_{acc}	Comment
				1	2	3	4			
Physics run	250	100	0.75	10	30	60	100	2.8	2.8	TDR nominal operation at 5Hz
Shutdown								1.5	4.3	Upgrade to full 500 GeV machine
Physics run	500	1000	1.8	10	30	60	100	5.5	9.8	TDR nominal operation at 5Hz
Physics run	350	200	1.	100	100	100	100	1.3	11.1	TDR nominal operation at 5Hz
Physics run	250	400	1.5	25	75	100	100	2.7	13.8	Operation at 10 Hz
Shutdown								1.5	15.3	Luminosity upgrade
Physics run	500	4500	3.6	10	50	100	100	9.3	24.6	TDR lumi–up at 5Hz

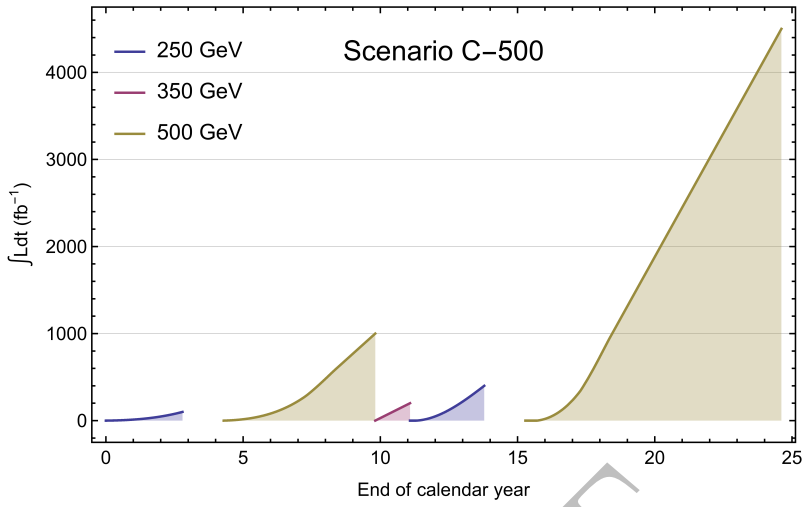

Figure 6: Accumulation of integrated luminosity versus real time for scenario C-500

Recent studies [5] have shown that a measurement of the Higgstrahlung cross section using the events with a Higgs recoiling from the hadronic decay of the Z boson (referred to as the hadronic recoil measurement) can be performed in a nearly model-independent way at $\sqrt{s} = 350\,\text{GeV}$, in the sense that detection efficiencies for SM Higgs decays differ by no more than 7%. This translates into a systematic error for the model-dependency of less than 11% of the statistical uncertainty [27]. Therefore we generally include the hadronic recoil measurements in the coupling fits.

Another method is to use the constraint $\sigma(ZH) = \sum_i \sigma(ZH) \cdot BR_i$, where the sum is over all Higgs decays, including Beyond the Standard Model (BSM) decays. This constraint is model independent if the measurement error for the branching ratio of BSM Higgs decays is included in the fit. If in the future an analysis can deliver a precision of $BR(H \to BSM) < 0.9\%$ at 95% C.L., then this constraint can lead to further improvements in the Higgs coupling precision [6].

With the currently available analyses, an initial long run at $\sqrt{s} = 250\,\text{GeV}$ benefits mostly the HZZ coupling. Most other couplings are limited by the knowledge of the HWW coupling or by statistics, and thus only reach their full potential once $\sqrt{s} \geq 350\,\text{GeV}$. Thus the overall physics output of a 250 GeV machine after 5 years of running will always be limited by the lack of sensitivity to the HWW coupling. In section 5, we will comment on the added physics value of starting ILC operation at $\sqrt{s} \geq 350\,\text{GeV}$.

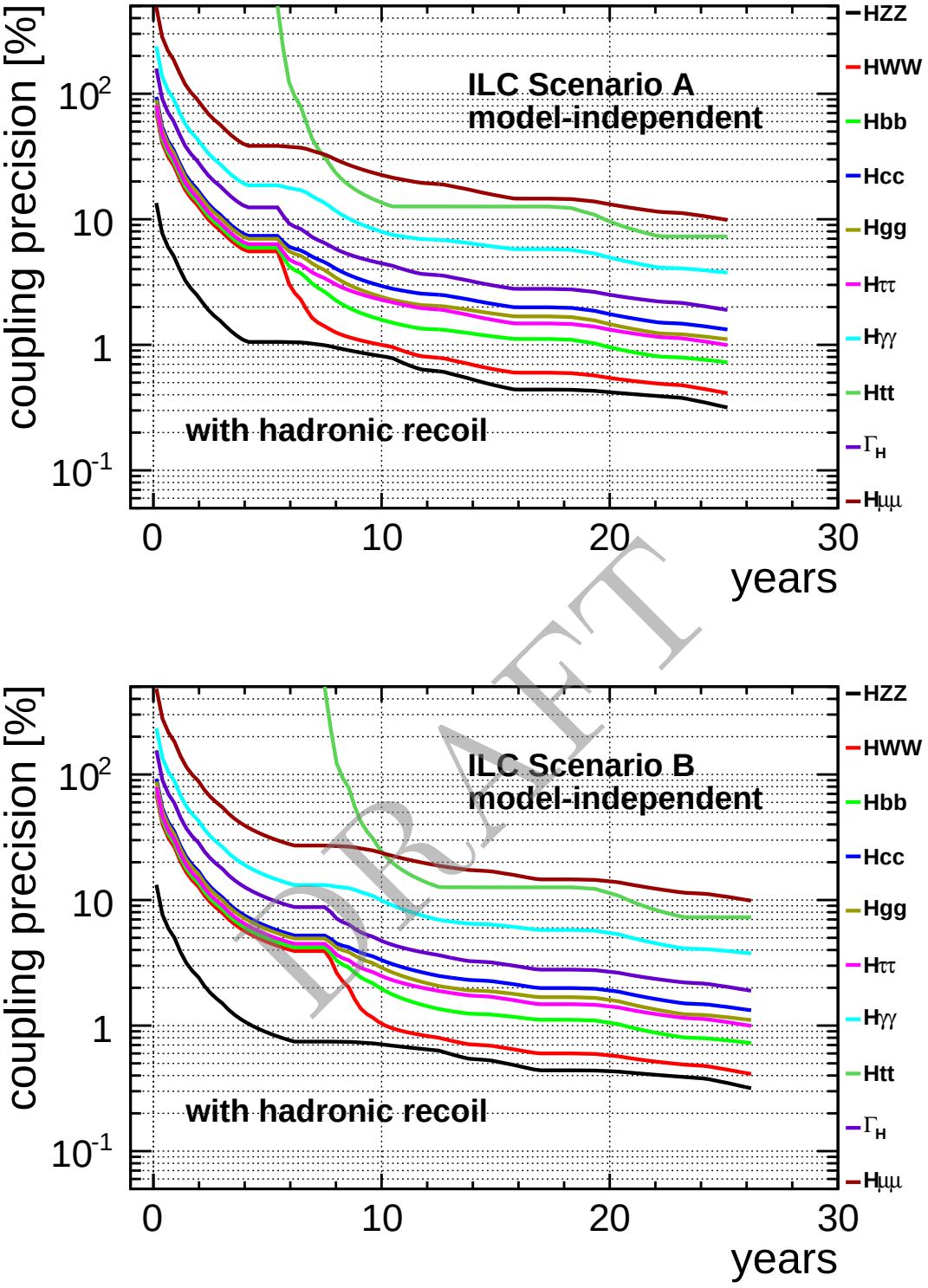

Figure 7: Time evolution of precision on various couplings of the Higgs boson in the scenarios A and B.

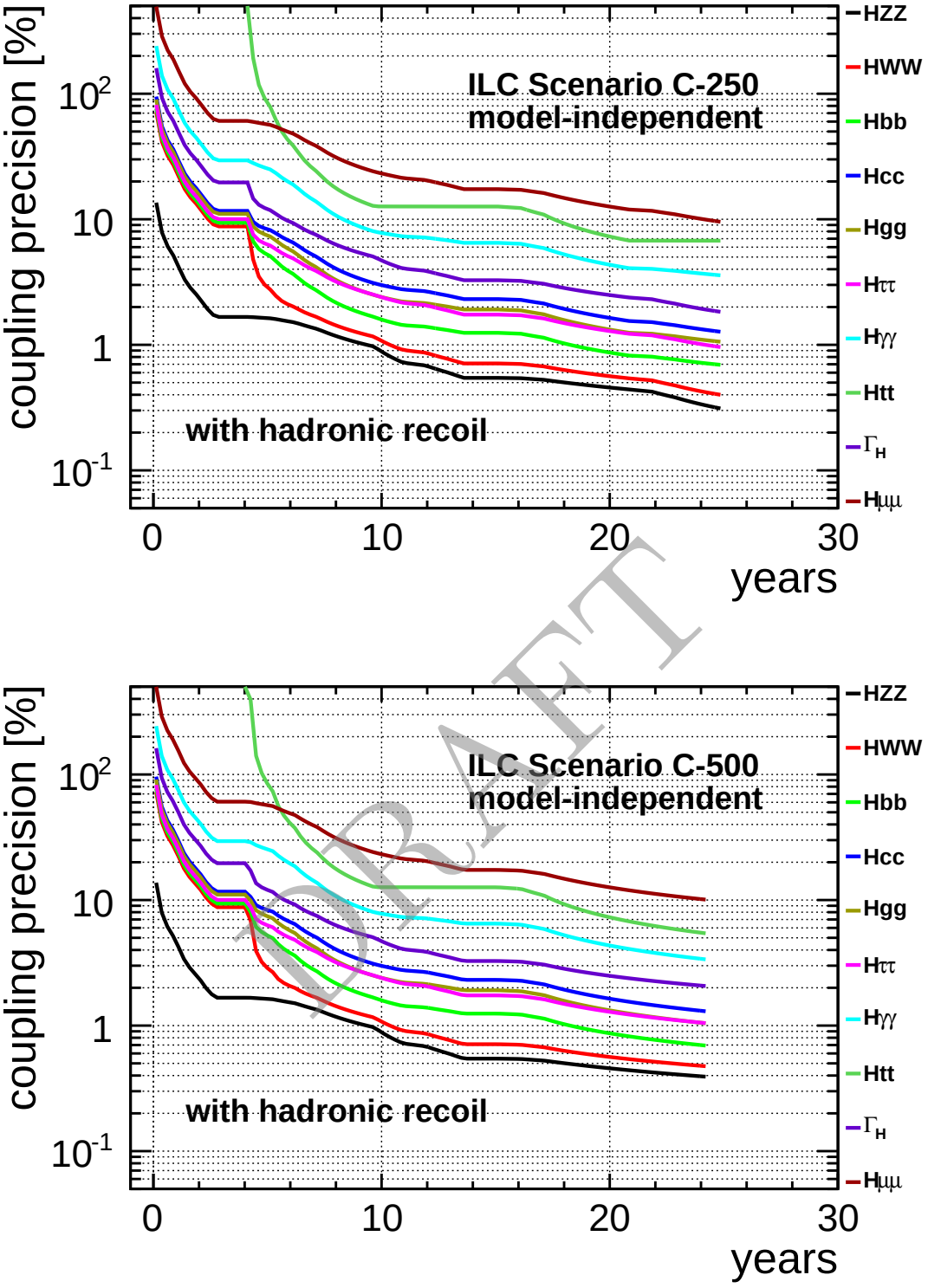

Figure 8: Time evolution of precision on various couplings of the Higgs boson in the C-250 and C-500 scenarios

4.2 Higgs mass

Besides being an important parameter of the Standard Model in its own right, the mass of the Higgs boson enters into the calculation of the phase space for Higgs decays, in particular for decays into WW and ZZ. Thus the uncertainty on the Higgs mass translates into a parametric uncertainty on the couplings extracted from the measurements of these decay modes. An uncertainty of $\delta M_H = 200\,\text{MeV}$ (the LHC expects to reach this level of precision or better [15]) has been estimated to cause an uncertainty of 2.2% and 2.5% on the partial widths of $H \to WW$ and $HH \to ZZ$, respectively [8]. If one would like to keep the parametric uncertainty on these observables at the level of 0.2%, $\delta M_H = 20\,\text{MeV}$ would be required. Currently the only way to reach this level of precision which has been demonstrated in full detector simulation is the Higgs recoil mass measurement with $Z \to \mu\mu$ at $\sqrt{s} = 250\,\text{GeV}$. With a momentum scale calibration from $Z \to \mu\mu$ at the Z pole and an in-situ beam energy calibration from $\mu\mu\gamma$ events, systematic uncertainties should be controlled at the 1 MeV level [9]. Figure 9 shows the luminosity scaling of Higgs recoil mass uncertainty. With $500\,\text{fb}^{-1}$ of data collected at $\sqrt{s} = 250\,\text{GeV}$, $\delta M_H = 25\,\text{MeV}$ is reached. In addition, preliminary studies of direct reconstruction of the Higgs mass from

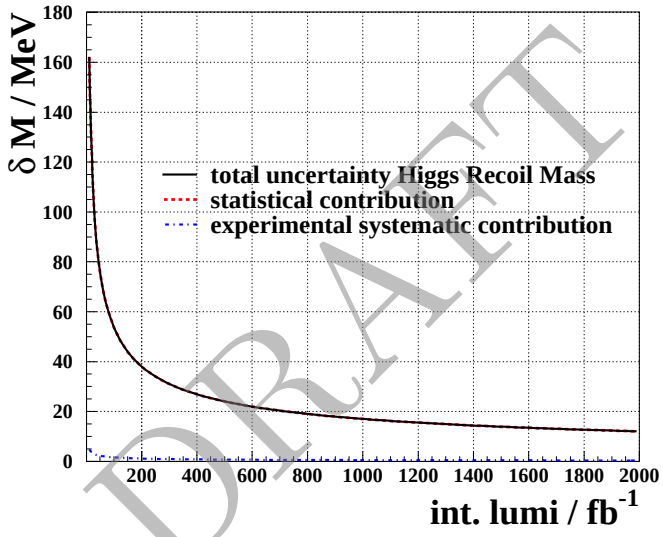

Figure 9: Luminosity scaling of the Higgs recoil mass measurement at $\sqrt{s} = 250$ GeV. Based on [10] and [9].

its decays to $b\bar{b}$ and WW at $\sqrt{s} = 500\,\text{GeV}$ show a competitive potential [9]. These studies should be substantiated in the future.

4.3 Electroweak couplings of the top quark

The precision measurement of the electroweak couplings of the top quark is a key item on the ILC physics program. It requires beam polarisation in order to disentangle the couplings to the Z boson and to the photon, which have different chiral properties. Besides being an important test of the Standard Model in its own right, the top quark couplings

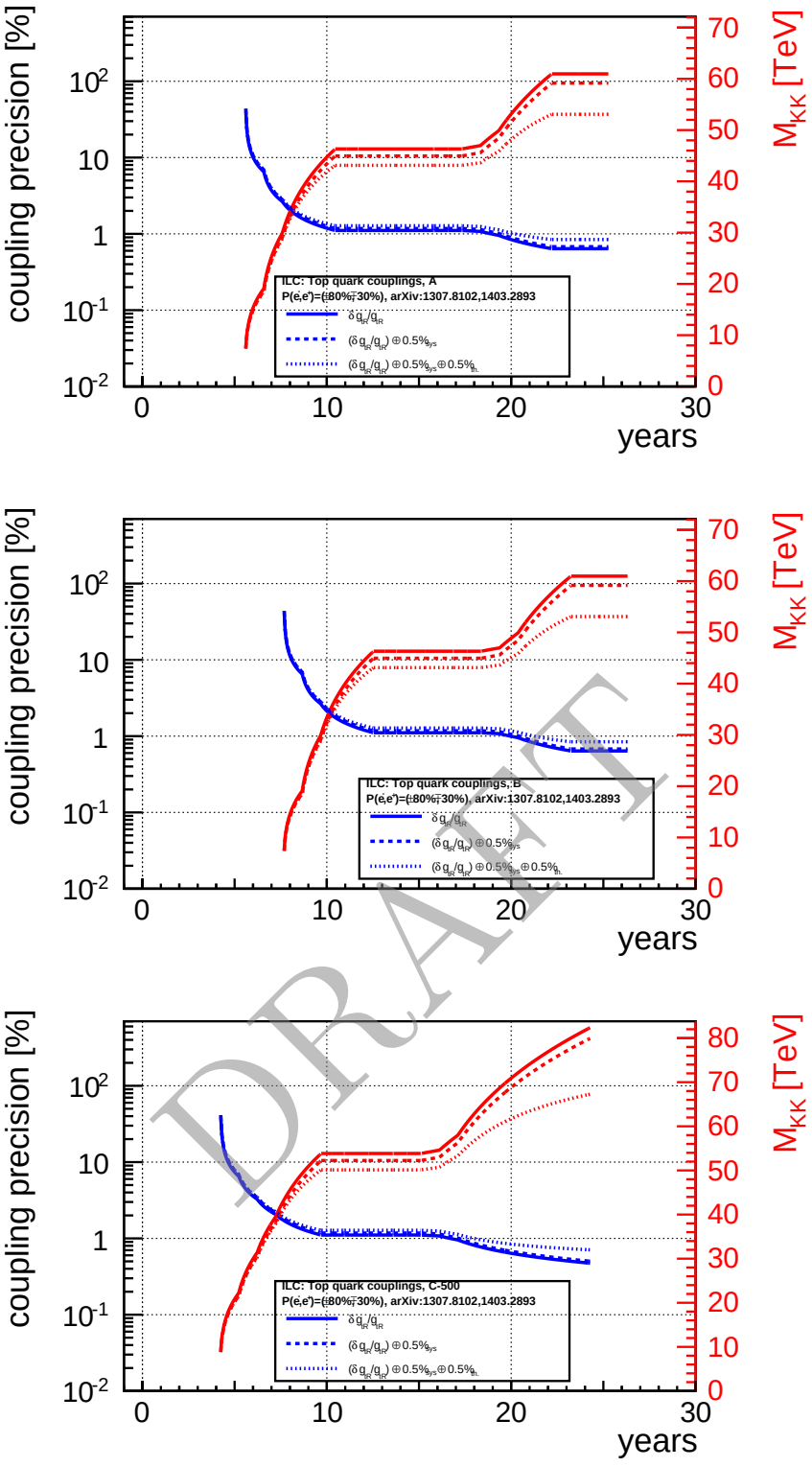

Figure 10: Time-evolution of right-handed top coupling and derived from this the sensitivity to the mass scale of Kaluza-Klein excitations in an extra-dimension model [12] for scenarios A, B and C-500.

are a prime indicator for physics beyond the SM. Due to its uniquely large mass and thus its particularly strong coupling to the Higgs boson there is a strong motivation to expect that new phenomena would become visible first in the top sector.

Figure 10 shows the time evolution expected for the right-handed top coupling based on [11]. It also shows as an example the sensitivity to the mass scale of new physics in a Extra-Dimension model derived from excluding deviations of the right-handed top coupling from its Standard Model prediction [12]. This indirect sensitivity for new physics can extend easily into the several-10-TeV regime, but requires at least $\sqrt{s} > 450\,\text{GeV}$.

4.4 Higgs Self-Coupling

The measurement of the Higgs self-coupling requires at least $\sqrt{s} \geq 450\,\text{GeV}$. A detailed study based on full simulation of the ILD detector concept at $\sqrt{s} = 500\,\text{GeV}$ originally assuming $m_H = 120\,\text{GeV}$ [13] has been updated recently [14] to $m_H = 125\,\text{GeV}$. Preliminary results have been obtained for both unlike-sign helicity configurations of the beams, showing a slight preference for right-handed electrons and left-handed positrons, which suppresses the background much stronger than the signal.

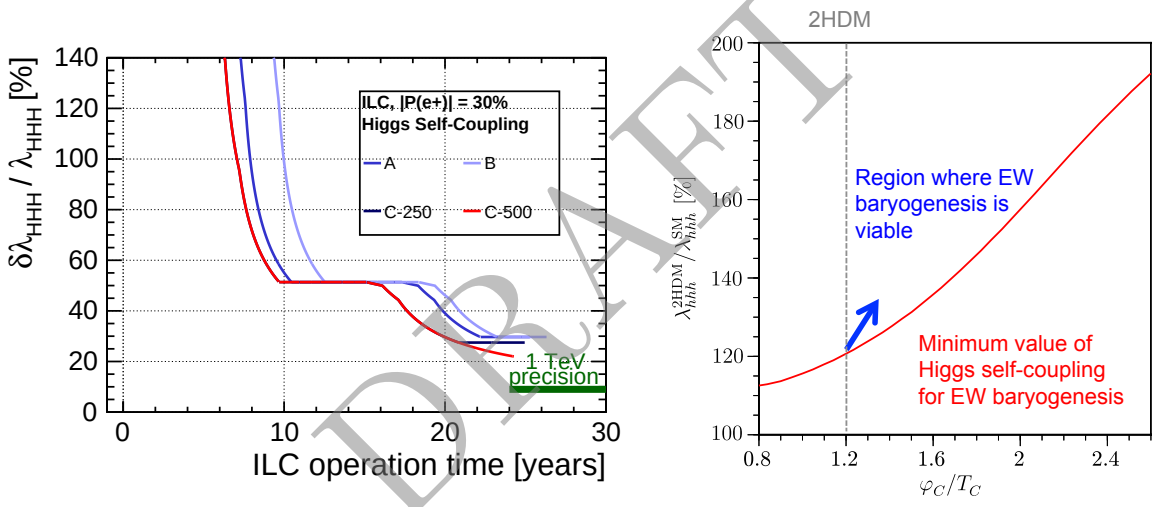

Figure 11: Left: Time evolution of the precision on the Higgs self-coupling for various running scenarios, based on the existing full simulation results exploiting the decay modes $H \to b\bar{b}$ and $H \to WW$, including an estimate of the effect of the ongoing analysis improvements (kinematic fitting, matrix element method, colour singlet jet clustering.) The green line shows for comparison the precision for the 1 TeV upgrade. Right: Example of allowed values of the Higgs self-coupling in Two-Higgs-Doublet-Models with electroweak baryogenesis normalised to the SM value [16]. The minimal deviation is in the order of 20%, but the Higgs self-coupling could also be twice as high as in the SM.

Figure 11 shows the time evolution of the precision on the Higgs self-coupling for the scenarios A, B, C-250 and C-500. The helicities are chosen according to table 2. At $\sqrt{s} = 500\,\text{GeV}$, the precision is modest, but for large integrated luminosities a precision

of 20% can be reached. This would clearly demonstrate the existance of the Higgs self-coupling, particularly when combined with possible future LHC results [15]. The green line indicates for comparison the precision that would be reached with the 1 TeV ILC upgrade Here, a precision of 10% or better can be reached.

These numbers can be contrasted with expectations from various extensions of the Standard Model. While only very small deviations are expected in the MSSM, deviations of 20% or more can be expected from models of electroweak baryogenesis [16].

4.5 Natural Supersymmetry: Light Higgsinos

Among of the prime motivations to expect physics beyond the Standard Model is the so-called hierarchy problem. It arises in the Standard Model since the mass of the Higgs boson as elementary scalar receives large corrections from quantum loops. Due to the large difference between the electroweak scale and the Planck scale, where gravity becomes strong, a fine-tuning of parameters to about 60 digits would be required in order to keep the Higgs boson mass close to the elctroweak scale, where it has been observed now by the LHC.

In Supersymmetry, the corresponding loop-diagrams with supersymmetric partner cancel the corrections, up to a small rest depending on the mass differences between the SUSY particles and their SM partners. If the masses of some SUSY particles become too large, again a certain amount of fine-tuning creeps in, albeit at much smaller levels than in the pure SM. SUSY models which try to minimize the amount of fine-tuning needed to stabilize the Higgs (and also the Z) boson mass have been titled "Natural Supersymmetry".

The most basic prediction of Natural SUSY models is that the lightest SUSY particles are a triplett of Higgsinos, whose mass is given by the non-SUSY-breaking parameter μ. The mass splitting within the triplet is inversly proportional to the SUSY-breaking gaugino mass parameter $m_{1/2}$. Coloured SUSY particles can be much heavier, with the $\tilde{t}_1$ mass between 1 and 2 TeV and the gluino mass in the $1.5 - 5$ TeV range [23].

It has been shown that these light Higgsinos can be observed at the ILC, including precise measurements of their propoerties [24]. At the LHC with $\sqrt{s} = 14$ TeV, they can be easily observed in cascade decays if the gluino is light enough, i.e. $m_{1/2} \lesssim 0.7$ TeV assuming gaugino mass unification, c.f. the left part of figure 12. This can be extended by same-sign dilepton In constrast, the range of the ILC is nearly independent of $m_{1/2}$, actually in the benchmark points studied in [24] $m_{1/2}$ was approximately 5 TeV. The green shaded area in indicates the region of parameter space in which the Dark Matter relic density is not larger than the observed value, while the read lines indicate the degree of fine-tuning (the lower Δ_{EW} the better). With $\sqrt{s} = 500$ GeV, the ILC and LHC14 together cover nearly all the region with a fine-tuning less than 30, while ILC with$\sqrt{s} =$ 1 TeV probes the region up to $\Delta_{EW} = 75$.

At the ILC, Higgsinos would be discovered very quickly once they are kinematically accessible. This is illustrated in the right part, which shows the discovery reach as a

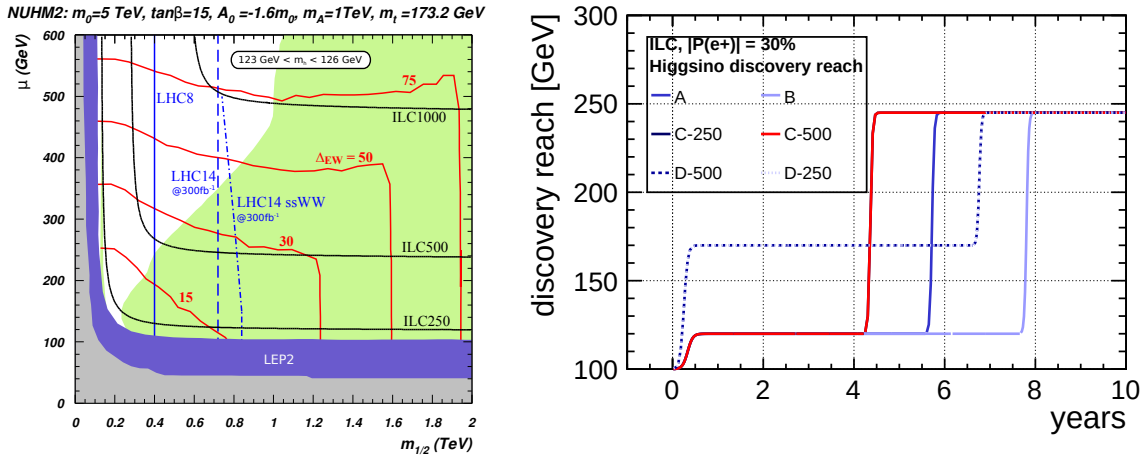

Figure 12: Left: Discovery reach of LHC and ILC in the μ vs $m_{1/2}$ plane. The ILC covers substancial parameter space with low fine-tuning inaccessible to the LHC. Further description see text. From [25]. Right: Time evolution of Higgsino discovery reach in different ILC running scenarios.

function of time for our running scenarios (for D-250 and D-500, c.f. section 5). With the integrated luminosities of the full ILC programm, the Higgsinos masses and cross-sections could then be measured to the level of 1% or better, which enables to prove that the discovered particles are indeed Higgsinos, to determine the parameters of the underlying model and e.g. to constrain the gaugino mass parameters even if they are in the multi-TeV regime. We point out that polarised beams are essential for this enterprise.

Obviously, reaching the highest possible center-of-mass energy as early as possible is desirable in terms of discovery potential of the machine, not only in case of Higgsinos, but also in view of other electroweak states with small mass differences which could espace detection at the LHC.

4.6 WIMP Dark Matter

One of the prime tasks of current and future colliders is to identify the nature of Dark Matter. WIMP Dark Matter can be searched for at colliders in a rather model-independent manner by looking for mono-jet or mono-photon events. Figure 13 compares actual LHC results, LHC projections and ILC projections. For the ILC, an integrated luminosity of $3.5\,\mathrm{ab}^{-1}$ is assumed at $\sqrt{s} = 500\,\mathrm{GeV}$, and the result is shown for different polarisation sharings. Note that data-taking with like-sign polarisation configurations is important in particular for the case of an axial-vector-type of interaction between the WIMPs and SM particles. For WIMP masses well below the kinematic limit, the reach in the effective operator scale (thus the scale of new physics) is basically independent of the WIMP mass.

Figure 14 shows the time evolution of the reach in new physics scale Λ in our running scenarios, taking as example the vector operator case and a WIMP mass of 10 GeV. Again it can be seen easily that early operation at high center-of-mass energies is preferred.

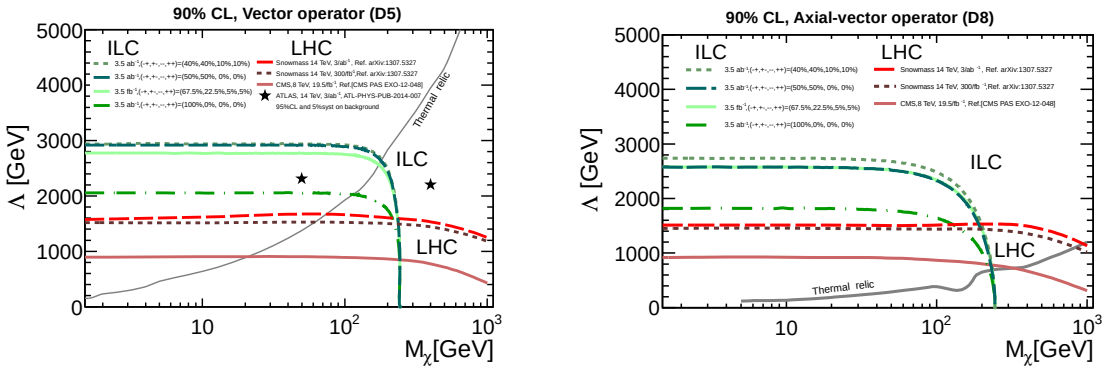

Figure 13: 90% CL reach for WIMP dark matter at LHC and ILC in the plane of effective operator scale vs WIMP mass. Left: For a vector operator mediating the WIMP interaction Right: For an axial-vector operator mediating the WIMP interaction

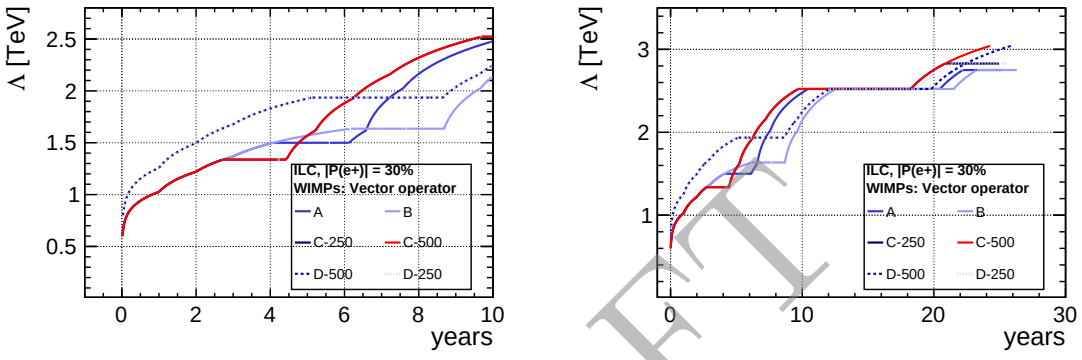

Figure 14: 90% CL reach for WIMP dark matter at ILC for a WIMP mass of 10 GeV in the vector operator case in our running scenarios. Left: zoom into the first 10 years Right: full running scenarios

5 Initial Operation at 350 GeV

Starting operations of the ILC at $\sqrt{s} = 350\,\text{GeV}$ offers a scientifically stronger initial physics program than starting at 250 GeV. At 350 GeV, Higgs production comes largely from the Higgstrahlung process ($e^+e^- \to ZH$), but the important WW-fusion process ($e^+e^- \to \nu_e\overline{\nu_e}H$) is rising by a factor of 3 w.r.t. $\sqrt{s} = 250\,\text{GeV}$, as illustrated in Figure 15. This enables precise measurements of both the Z-Higgs coupling (Δg_{HZZ}) and the W-Higgs coupling (Δg_{HWW}). These critical measurements are important to the determination of the total Higgs width (Γ_H), and the most precise model independent determination of all the couplings, testing the standard model, and measuring invisible or exotic decays of the Higgs boson.

At 250 GeV, the Higgs recoil mass calculation from the $Z \to \mu^+\mu^-$ decay allows the Z-Higgs coupling to be precisely measured ($\Delta g_{HZZ} \sim 1.3\%$) and the Higgs mass is measured with a precision of ~ 35 MeV or better (see Section 4.2 for a discussion of the precision versus integrated luminosity). Theoretical motivations require $\Delta m_H < 50$ MeV. However, at $\sqrt{s} = 250$ GeV, the cross section for the important WW-fusion process ($e^+e^- \to \nu_e\overline{\nu_e}H$)

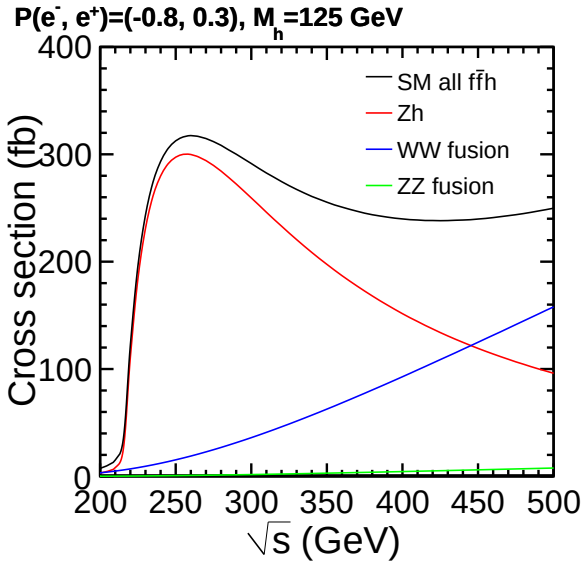

Figure 15: Cross-section for Higgs production in Higgstrahlung and WW-fusion as a function of $\sqrt{s}$. From [3].

is small, limiting the Higgs coupling measurements, in particular the W-Higgs coupling (g_{HWW}) and the total width of the Higgs boson (Γ_H). For the best precision on Higgs properties, a larger WW-fusion rate is needed, which comes with running at ~ 350 GeV or higher.

In order to illustrate this, we also studied two scenarios D-250 and D-500, defined in figure 16. These are defined analogously to scenarios C-250 and C-500, but start with collecting an integrated luminosity of 500 fb^{-1} at $\sqrt{s} = 350$ GeV, followed by an energy upgrade to $\sqrt{s} = 500$ GeV. After collecting 1 ab^{-1} at 500 GeV machine is then operated at $\sqrt{s} = 250$ GeV in 10-Hz-mode, collecting 500 fb^{-1}. Like in scenarios C-X, this is followed by a luminosity upgrade. Table 6 summarizes the total integrated luminosities at each energy for the D-X scenarios in comparison to the A-C scenarios, and Figure 16 shows their time evolution details.

	$\int \mathcal{L}dt$ [fb^{-1}]				
$\sqrt{s}$	A/B	C-250	D-250	C-500	D-500
250 GeV	2000	2000	2000	500	500
350 GeV	200	200	500	200	500
500 GeV	3000	3500	3500	5500	5500

Table 6: Proposed total target integrated luminosities for $\sqrt{s} = 250, 350, 500$ GeV in all scenarios.

Figure 17 shows the corresponding evolutions of the Higgs couplings from the fully model-independent fit, including the hadronic recoil measurements. In comparison to the time evolutions shown in section 4.1, there is a significant improvement in the early performance of the machine, since not only the Z-Higgs coupling, but also the W-Higgs coupling reaches a 1% precision in the first 5 years.

	E_{CM}	$\int$Ldt	L_{peak}	Ramp				T	T_{acc}	Comment
				1	2	3	4			
Physics run	350	500.	1.	10	30	60	100	5.2	5.2	TDR nominal operation at 5Hz
Shutdown								1.2	6.4	Upgrade to full 500 GeV machine
Physics run	500	1000	1.8	10	50	100	100	4.9	11.3	TDR nominal operation at 5Hz
Physics run	250	500	1.5	25	75	100	100	3.1	14.4	Operation at 10Hz
Shutdown								1.5	15.9	Luminosity upgrade
Physics run	500	2500	3.6	10	50	100	100	5.8	21.7	TDR lumi-up at 5Hz
Physics run	250	1500	3.	25	75	100	100	4.2	25.9	TDR lumi-up at 10Hz

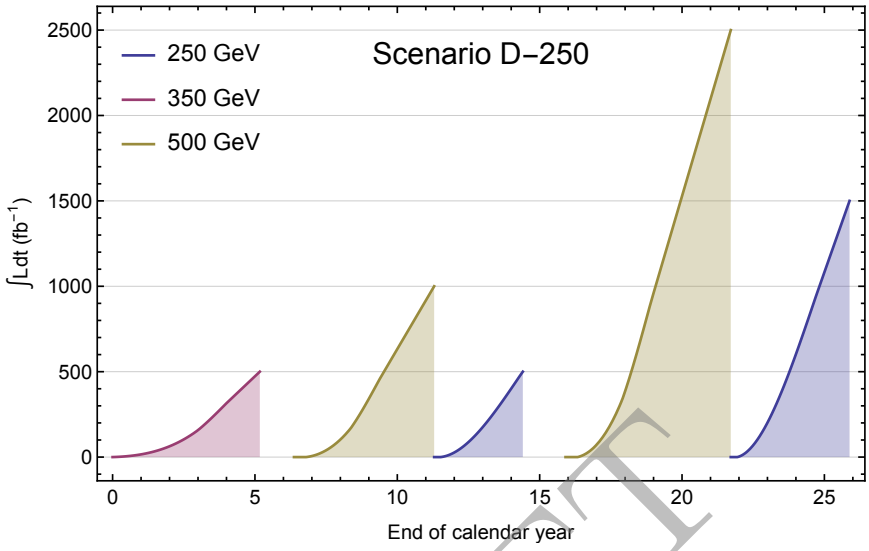

	E_{CM}	$\int$Ldt	L_{peak}	Ramp				T	T_{acc}	Comment
				1	2	3	4			
Physics run	350	500.	1.	10	30	60	100	5.2	5.2	TDR nominal operation at 5Hz
Shutdown								1.2	6.4	Upgrade to full 500 GeV machine
Physics run	500	1000	1.8	10	50	100	100	4.9	11.3	TDR nominal operation at 5Hz
Physics run	250	500	1.5	25	75	100	100	3.1	14.4	Operation at 10Hz
Shutdown								1.5	15.9	Luminosity upgrade
Physics run	500	4500	3.6	10	50	100	100	9.3	25.2	TDR lumi-up at 5Hz

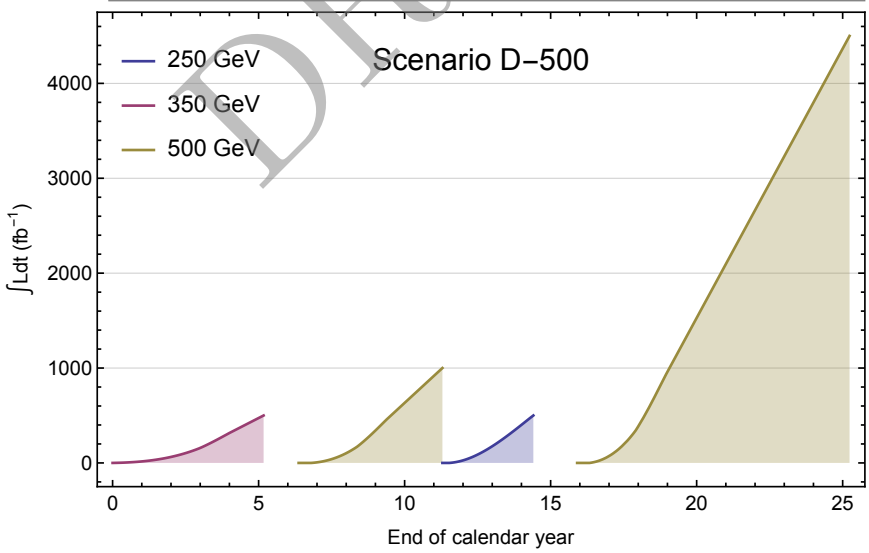

Figure 16: Definition of the D-250 and D-500 scenarios.

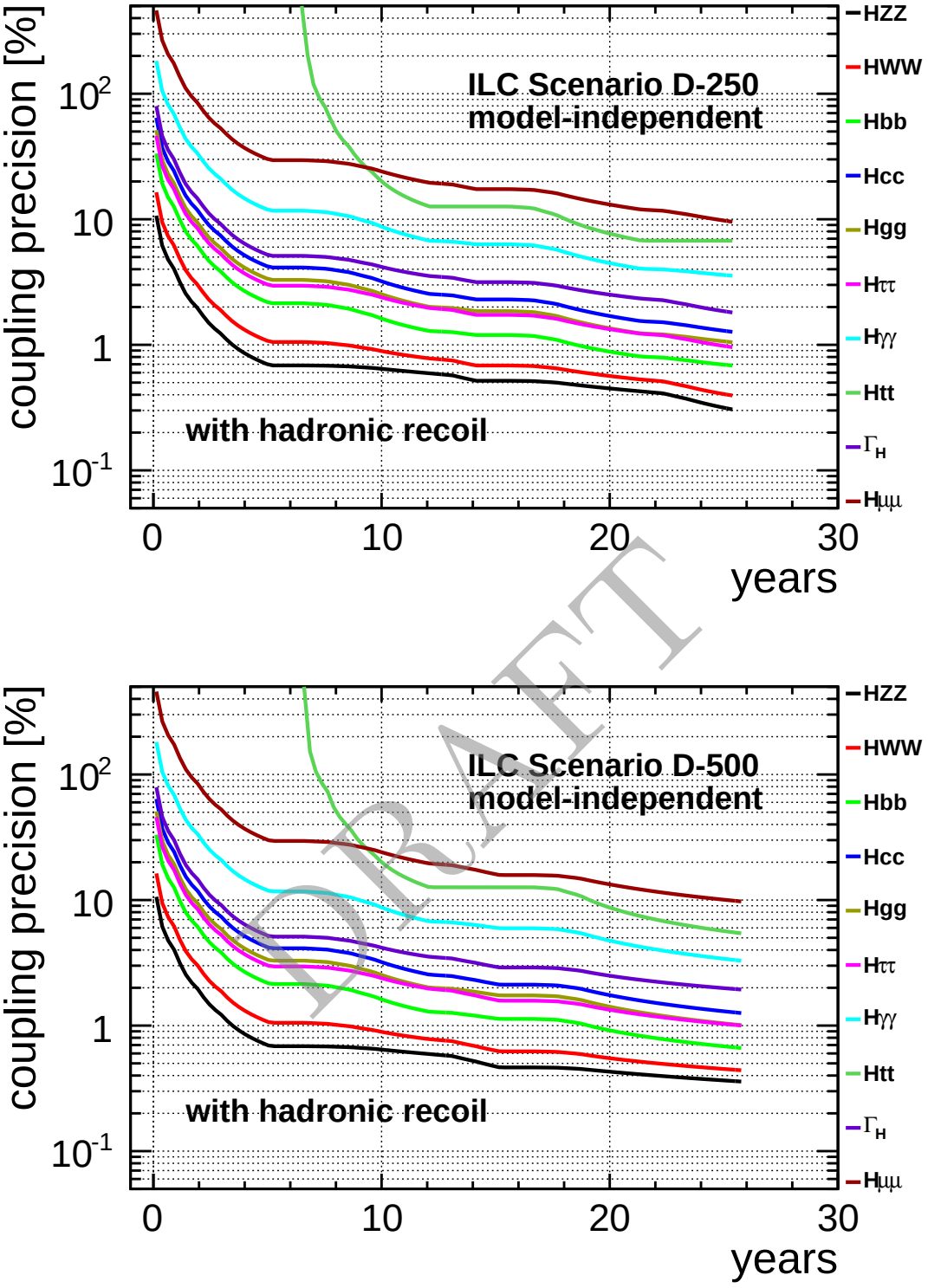

Figure 17: Time evolution of precision on various couplings of the Higgs boson in the D-250 and D-500 scenarios

In addition to the significantly improved Higgs coupling measurements at 350 GeV compared to 250 GeV, top pair production is open, providing another compelling physics channel of investigation. The top mass can be measured precisely to the theoretically interesting < 100 MeV level and QCD effects in the $t\bar{t}$ system can be studied. This effect can only be studied close to threshold, not in the continuum, and provides important input to the extraction of the top Yukawa coupling at higher energies, where similar threshold effects exist. In addition, indirect searches for new physics e.g. via charged triple gauge couplings, and direct searches, e.g. for Dark Matter particles, will profit immensely from the higher centre-of-mass energy.

The main arguments for operating the ILC at $\sqrt{s} = 250$ GeV are the model-independent measurements of the Higgs mass and the total Higgsstrahlung cross-section via the recoil against a leptonically decaying Z boson. These measurements perform worse at higher energies, since the decay leptons of the Z boson are more energetic, and in particular in the golden $Z \to \mu\mu$ mode the measurement suffers from the degraded momentum resolution. This is most relevant for an ultra-precise measurement of the Higgs mass. However this precision is not needed before the cross-section times branching ratio measurements reach the $\sim 1\%$ level, c.f. the discussion in section 4.2. Therefore, from the point of view of optimising the early physics output of the machine, the ultra-precise Higgs mass measurement can be done at a later stage. According to Figure 9, a dataset of $500 - 700\,\text{fb}^{-1}$ should be sufficient to reach $25 - 20$ MeV precision on the Higgs mass. Such a run is included in the D-X scenarios after the first 500 GeV run.

For the cross-section measurement, the picture changes significantly due to the hadronic decay modes of the Z bosons. Today's understanding is that with the excellent reconstruction capabilities of the ILC detectors for hadronic final states, the hadronic modes can be exploited with a very small residual model-dependency of about half the statistical uncertainty (see also the discussion in section 4.1). Here, the additional boost of the Z and the Higgs at higher $\sqrt{s}$ even makes this measurement easier, since the jets become more separated.

Figure 18 directly compares the time evolution of Δg_{HZZ} and Δg_{HWW} for the case including the hadronic recoil. While the gain in early precision on Δg_{HWW} is obvious, it should be noted that due to the hadronic recoil the initial 350 GeV running is superior to 250 GeV running even concerning Δg_{HZZ}.

Figure 19 shows the analoguous comparison of all scenarios for Δg_{Hbb} and Δg_{Hcc} for the case including the hadronic recoil. Also here, a clear gain in early precision is visible when starting at $\sqrt{s} = 350$ GeV.

In contrast, Figures 20 and 21 show the time evolutions of Δg_{HZZ}, Δg_{HWW}, Δg_{Hbb} and Δg_{Hcc} with the additional constraint that all branching fractions add up to 100%. As discussed in section 4.1) such a constraint is model indepedent so long as the measurment error for BSM decays is included in the fit. This figure assumes that a future analysis of BSM decays gives $BR(H \to BSM) < 0.9\%$ at 95% C.L.

The Higgs coupling precision for the first five years of ILC running are shown in Table 7 for Scenarios B and D-500, along with the expected final results for HL-LHC.

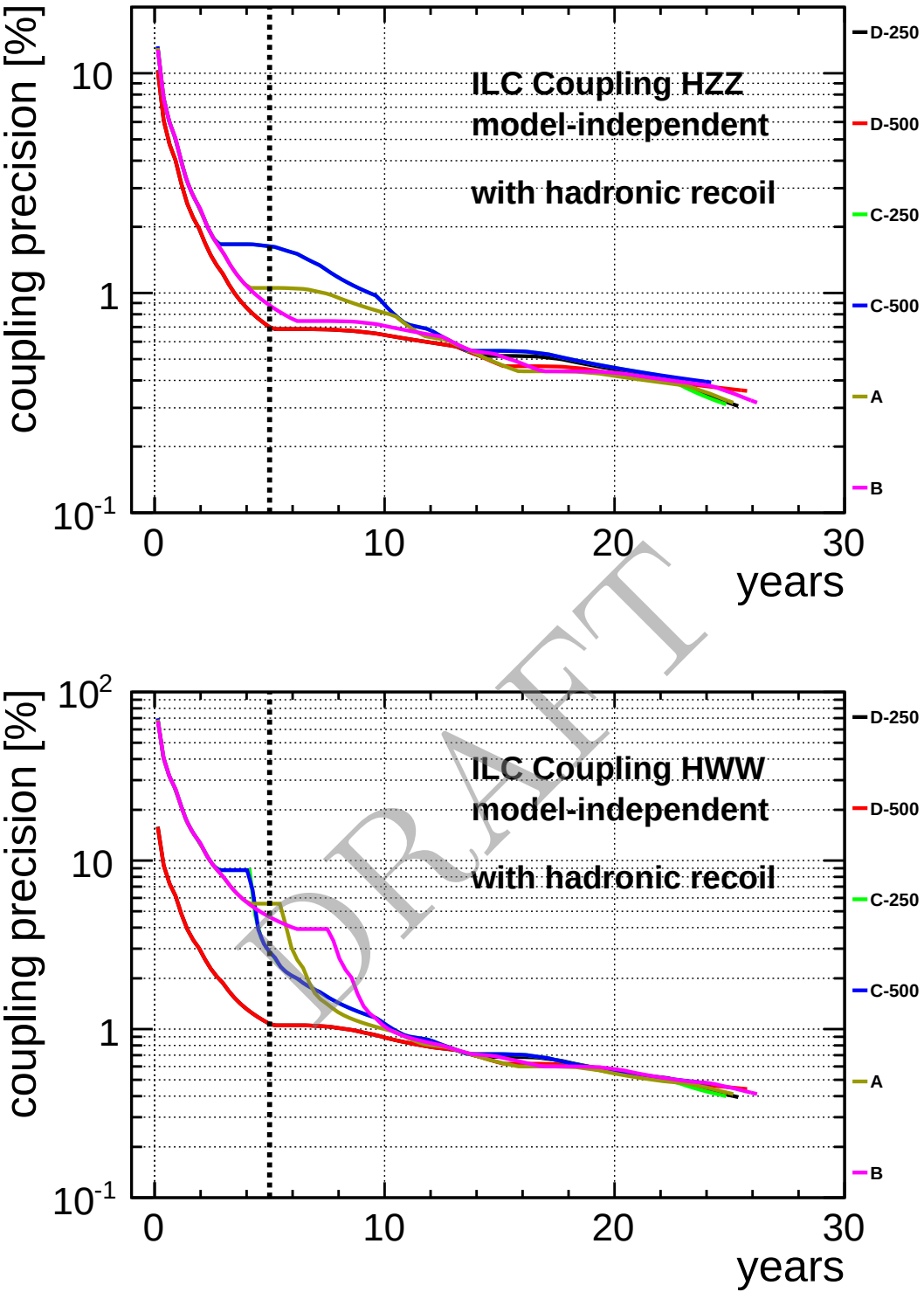

Figure 18: Time evolution of precision on the Z-Higgs and W-Higgs couplings in all scenarios, including the hadronic recoil measurements.

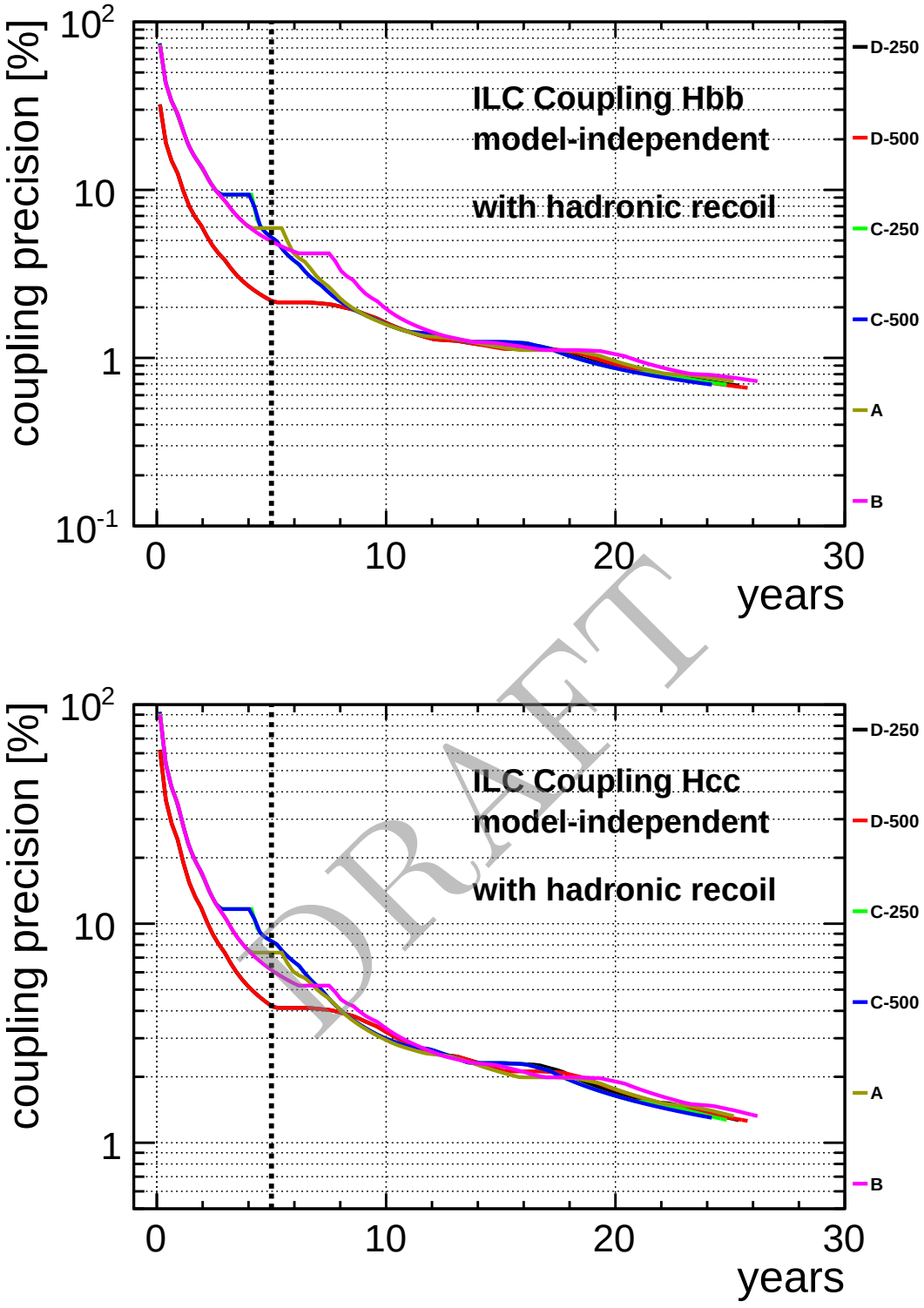

Figure 19: Time evolution of precision on the b-Higgs and c-Higgs couplings in all scenarios, including the hadronic recoil measurements.

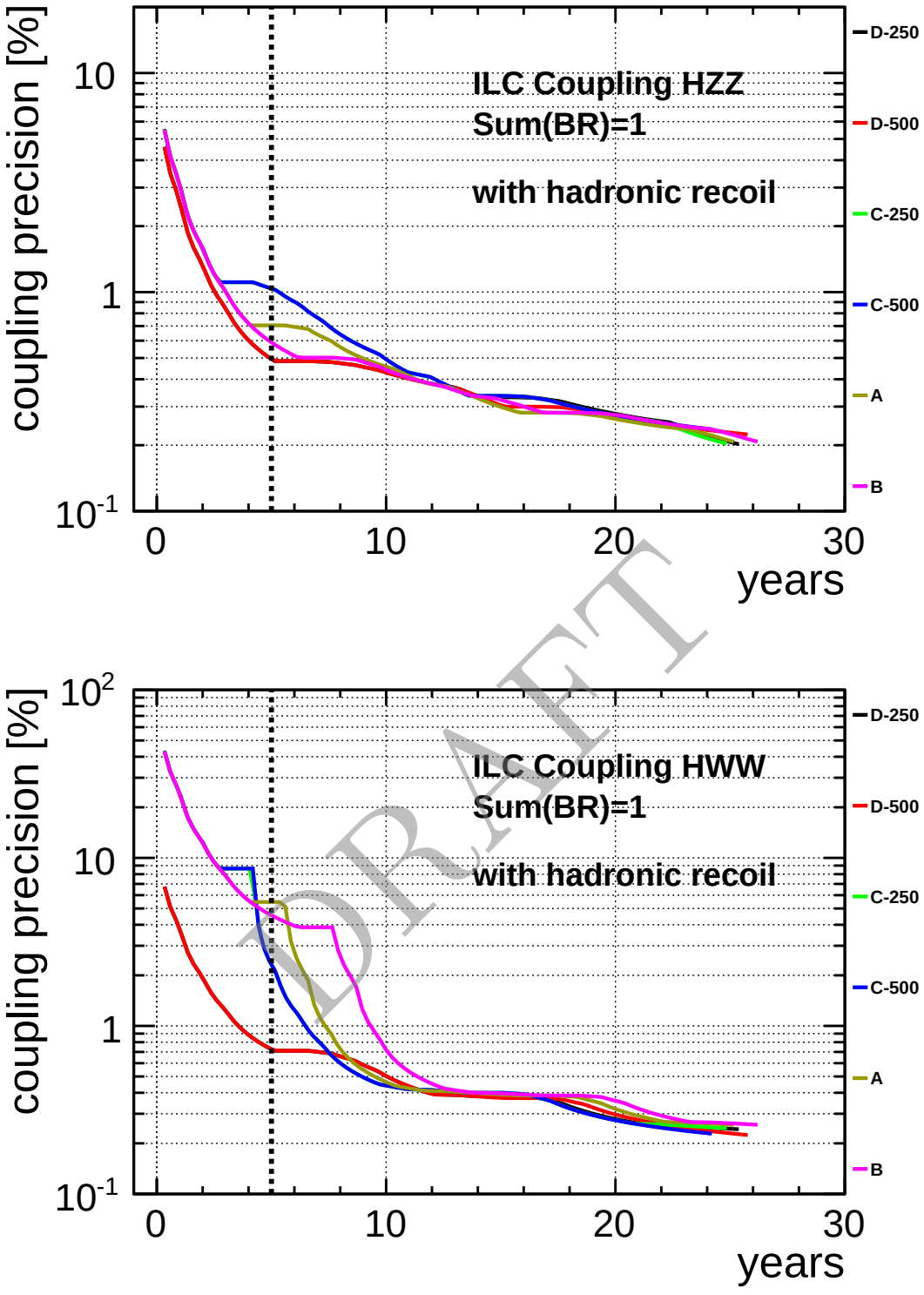

Figure 20: Time evolution of precision on the Z-Higgs and W-Higgs couplings in all scenarios, assuming $\sum BR = 1$.

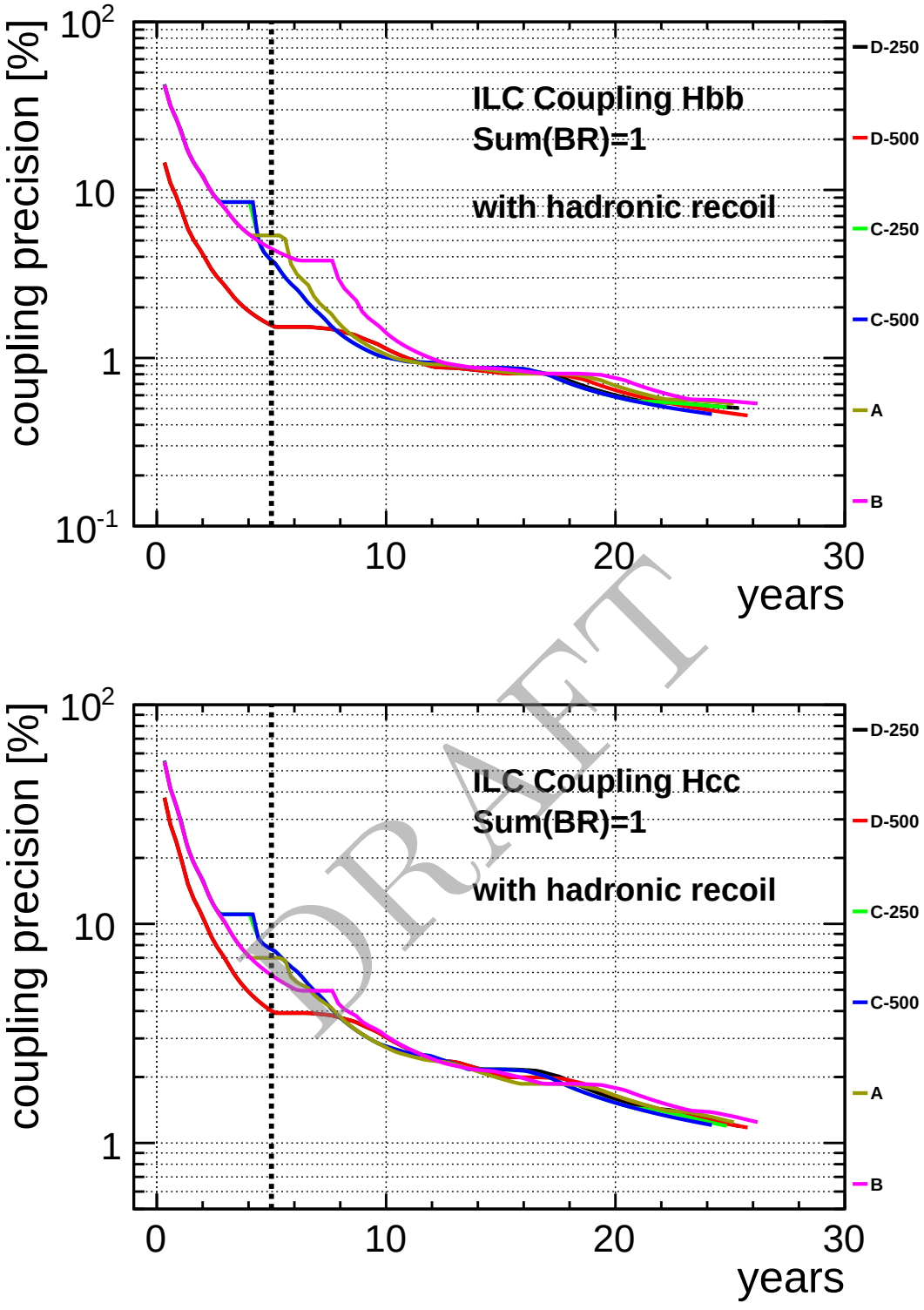

Figure 21: Time evolution of precision on the b-Higgs and c-Higgs couplings in all scenarios, assuming $\sum BR = 1$.

	HL-LHC	ILC Scenario B	ILC Scenario D-500
$\sqrt{s}$ (GeV)	1400	250	350
L (fb^{-1})	3000	360	470
$\gamma\gamma$	2-5 %	14.8 %	10.9 %
gg	3-5 %	4.8 %	2.9 %
WW	2-5 %	3.9 %	0.63 %
ZZ	2-4 %	0.63 %	0.49 %
$t\bar{t}$	7-10 %	5.3 %	3.7 %
$b\bar{b}$	4-7 %	3.8 %	1.3 %
$\tau^+\tau^-$	2-5 %	4.3 %	2.4 %
$\Gamma_T(h)$	5-8 %	7.3 %	2.1 %

Table 7: Expected accuracies $\Delta g_i/g_i$ of Higgs boson couplings for the end of the HL-LHC program and for the first five years of ILC running assuming either Scenario B or Scenario D-500. The couplings are derived from a seven parameter fit of $g_g, g_\gamma, g_W, g_Z, g_b, g_t, g_\tau$ using the model dependent constraints described in Section 10.3.7 of the first report of the LHC Higgs Cross Section Working Group [26]. The HL-LHC coupling errors are taken from the 2013 Snowmass Higgs Working Group Report [15].

$BR(H \to BSM)$	no measurement		$< 0.9\%$ at 95 % CL	
	Scenario B	Scenario D-500	Scenario B	Scenario D-500
$\sqrt{s}$ (GeV)	250	350	250	350
L (fb^{-1})	360	470	360	470
$\gamma\gamma$	14.9 %	11.0 %	14.8 %	10.9 %
gg	5.2 %	3.1 %	4.9 %	2.9 %
WW	4.0 %	1.0 %	3.9 %	0.67 %
ZZ	1.1 %	0.72 %	0.66 %	0.51 %
$b\bar{b}$	4.4 %	2.0 %	3.9 %	1.4 %
$\tau^+\tau^-$	4.7 %	2.8 %	4.3 %	2.5 %
$c\bar{c}$	5.6 %	3.9 %	5.3 %	3.7 %
$\Gamma_T(h)$	9.6 %	4.9 %	7.4 %	2.5 %

Table 8: Model independent Higgs boson coupling errors $\Delta g_i/g_i$ for the first five years of ILC running assuming either Scenario B or Scenario D-500. The constraint $\sum_i BR_i = 1$ is model independent if the measurement error for the branching ratio of beyond standard model (BSM) Higgs decays is included in the fit; results are shown for no measurement and for a hypothetical future limit of $BR(H \to BSM) < 0.9\%$ at 95% C.L.

Model independent results for the first five years of ILC running for Scenarios B and D-500 are shown in Table 8.

Considering these factors, the physics program for a initial program at $\sqrt{s} = 350\,\text{GeV}$ is significantly stronger than the comparable program starting from $\sqrt{s} = 250\,\text{GeV}$.

6 Maximum centre-of-mass energy reach of ∼500 GeV ILC and the top Yukawa coupling

The top Yukawa coupling is measured at the ILC from the process $e^+e^- \to t\bar{t}h$, which opens kinematically at around $\sqrt{s} = 475\,\text{GeV}$. Full detector simulation studies showed that at $\sqrt{s} = 500\,\text{GeV}$, the top Yukawa coupling can be determined with a precision of 9.9% based on an integrated luminosity of $1\,\text{ab}^{-1}$ with $P(e^-, e^+) = (-80\%, +30\%)$ [22]. In terms of the running scenarios proposed in this doument, this translates into final precisions between 5% and 7%, c.f. Figures 7 and 8.

Figure 22 shows the relative cross section for $t\bar{t}h$ production as a function of $\sqrt{s}$, which shows that it is still steeply rising at $\sqrt{s} = 500\,\text{GeV}$, increasing nearly four-fold by $\sqrt{s} = 550\,\text{GeV}$. Since at the same time the main backgrounds, e.g. from non-resonant tbW and $t\bar{t}b\bar{b}$ production, decrease, the precision on the top Yukawa coupling improves by better than a factor of two w.r.t. $\sqrt{s} = 500\,\text{GeV}$ for the same integrated luminosity. This significant improvement in the important top Yukawa coupling parameter motivates serious consideration of extending the upper center-of-mass reach of the nominally 500 GeV ILC to about 550 GeV.

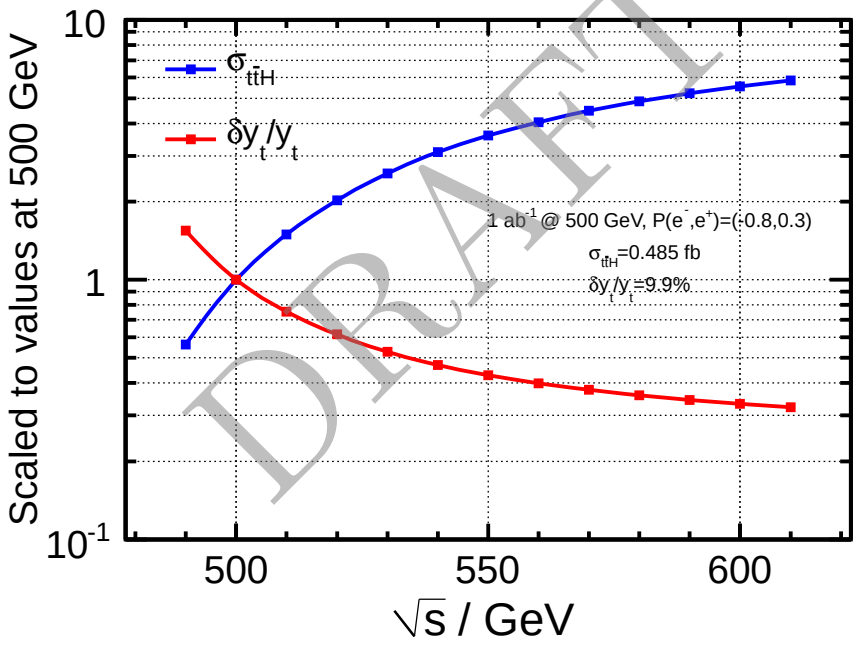

Figure 22: Relative cross section and top Yukawa coupling precision versus centre-of-mass energy, extrapolated based on scaling of signal and main background cross-sections.

7 Other Centre-of-Mass Energies

$\sqrt{s} \gtrapprox 2M_{new-particle}$

With the discovery of a new pair-produced particle at the upcoming running of the LHC or the early operations of the ILC, the ILC will operate in follow-up studies at or near the threshold for the production of this new particle to determine it detailed properties, including spin and mass, as well as mixing angles and complex phases in specific cases.

$\sqrt{s} = 1\,\textbf{TeV}$

As already pointed out above in case of the Higgs self-coupling, an extension of the ILC to $\sqrt{s} = 1\,\text{TeV}$ offers significant improvements for many Standard Model precision measurements including the Higgs boson properties. In addition it immensely enlarges the reach of the ILC for direct production of new particles, in particular Dark Matter candidates. Therefore, the compatibility of the ILC baseline design with a later upgrade to 1 TeV should be preserved.

WW-threshold, Z-pole for physics, Z-pole for calibration

Beyond the physics goals in the 250-500 GeV energy range that have primarily been the focus of the discussion in the previous sections, lower energy operation of the ILC must be considered for a number of important purposes:

1. Precision measurements of the W boson mass at the W pair threshold near $\sqrt{s} =$ 161 GeV could reach the few MeV regime. This measurement is qualitatively unique since it is subject to orthogonal experimental systematic uncertainties compared to kinematic reconstruction of the W mass in the continuum, and since it has a direct theoretical interpretation.

2. Ultra-precise measurement of the left-right asymmetry (A_{LR}) in the production of Z bosons at $\sqrt{s} = M_Z$ based on 10^9 Z decays (so-called Giga-Z) offers an important update of the SLD measurements of A_{LR} and its tension with the LEP forward-backward asymmetry measurements.

3. Operation of the ILC at $\sqrt{s} = M_Z$ also offers a valuable calibration tool even at lower luminosities than those required for the Giga-Z measurement. However the experiments should quantify their needs more precisely.

$\sqrt{s}$	1 TeV	90 GeV	160 GeV
$\int \mathcal{L}dt$ [fb^{-1}]	8000	100	500

Table 9: Proposed total target integrated luminosities for other $\sqrt{s}$

Target Integrated Luminosities and Polarisation Splitting

Table 9 shows proposed total target integrated luminosities for further options of the ILC program, in particular the 1 TeV upgrade, precision measurements at the Z pole and a W pair production threshold scan for a precision measurement of the W mass. The luminosities given here serve as guideline for future physics studies of these options.

Tables 10 suggests a luminosity sharing between the beam helicity configurations for these energies, while and 11 gives the corresponding absolute integrated luminosities per helicity configuration.

	fraction with sgn$(P(e^-), P(e^+)) =$			
	(-,+)	(+,-)	(-,-)	(+,+)
$\sqrt{s}$	[%]	[%]	[%]	[%]
1 TeV	40	40	10	10
90 GeV	40	40	10	10
160 GeV	67.5	22.5	5	5

Table 10: Relative sharing between beam helicity configurations proposed for low energy and 1 TeV running.

	integrated luminosity with sgn$(P(e^-), P(e^+)) =$			
	(-,+)	(+,-)	(-,-)	(+,+)
$\sqrt{s}$	[fb^{-1}]	[fb^{-1}]	[fb^{-1}]	[fb^{-1}]
1 TeV	3200	3200	800	800
90 GeV	40	40	10	10
160 GeV	340	110	25	25

Table 11: Integrated luminosities per beam helicity configuration resulting from the fractions in table 10

The exact priority of the low energy runs will largely depend on the future results of the LHC and the first round of ILC operation. The longer a direct discovery of new physics evades experimental proof, the more relevant ultra-precise measurements of the most fundamental parameters of the Standard Model will become.

8 Conclusions

This report summarizes studies of possible staging scenarios for the ILC. The ILC TDR proposes building a full 500 GeV collider from the start and this remains the preferred

construction plan for realizing the ILC. However, it may be necessary to reach 500 GeV only after staging the construction from a lower energy. In each of the primary scenarios considered here, the machine was assumed to first be built for 250 GeV, and subsequently upgraded to ∼500 GeV after operation at 250 GeV for a variable period depending on the particular scenario. A special study was done for a secondary scenario in which the intial phase of staging was at 350 GeV.

From this study we have reached the following conclusions:

- The optimal scenario starting from 250 GeV is C-500, which spends the largest fraction of its lifetime operating at the highest possible energy. This scenario optimizes the possibility of discoveries of new physics while making the earliest measurements of the important Higgs properties.
- A significant improvement in the earliest physics reach can be achieved if the first phase of the collider is at 350 GeV, rather than 250 GeV. This would optimize the Higgs measurements as well as open up measurements of the top mass and electroweak couplings.
- The physics impact of the ILC is significantly improved if the maximum energy of the ∼500 GeV ILC is stretched to ∼550 GeV where the top Yukawa precision is more than a factor of two times better than at 500 GeV.

Future investigations should include the following:

- The reduction in physics which would result if the assumed 30% position polarization were reduced to zero.
- The importance of the Z-pole calibration referred to in Section 7
- The capability of ILC detectors to operate with 10 Hertz collisions.

This report emphasizes the physics that we are absolutely certain will be done with the ILC and the operational accelerator plans for achieving the best outcomes for that physics. This physics includes precision measurements of the Higgs boson, the top quark, and possibly measurements of the W and Z gauge bosons. While this certain program provides a compelling and impactful scientific outcome, discoveries by the LHC or the early running of the ILC could significantly expand the scientific impact of the ILC. There are existing scientific motivations to anticipate such possibilities. Such discoveries could alter the run plan from that described here, as operations at our near the threshold of a pair-produced new particle, for example, would be added, a capability that is one of the particular operational strengths of the ILC.

Acknowledgement

Many members of the ILC community contributed to this report by valuable discussions as well as sharing of results and code. In particular we'd like to thank Mikael Berggren, Roberto Contino, Christophe Grojean, Benno List, Maxim Perelstein, Michael Peskin, Roman Pöschl, Juergen Reuter, Tomohiko Tanabe, Mark Thomson, Junping Tian, Graham Wilson and all members of the ILC Physics Working Group.

References

[1] R. D. Heuer et al., "Parameters for the Linear Collider," Update November 20, 2006, http://ilc-edmsdirect.desy.de/ilc-edmsdirect/file.jsp?edmsid=*948205. Prepared by the parameters sub-panel of the International Linear Collider Steering Committee.

[2] Dugan, Harrison, List and Walker, "Implications of an Energy-Phased approach to the realization of the ILC," February 11, 2014.

[3] H. Baer *et al.*, "The International Linear Collider Technical Design Report - Volume 2: Physics," arXiv:1306.6352 [hep-ph].

[4] K. Seidel, F. Simon, M. Tesar and S. Poss, Eur. Phys. J. C **73** (2013) 2530 [arXiv:1303.3758 [hep-ex]].

[5] M. Thomson and K. Mei, "Visible and Invisible Higgs Decays at 350 GeV", presentation at Americas Workshop on Linear Colliders, Fermilab, Batavia IL, USA, May 12-16, 2014, `http://agenda.linearcollider.org/getFile.py/access?contribId=172&sessionId=14&resId=0&materialId=slides&confId=6301`
and update: M. Thomson, "Higgs physics - where ar we, what is missing," presentation at the ILD meeting 2014, Oshu City, Japan, Sept. 6-9 2014, `https://agenda.linearcollider.org/getFile.py/access?contribId=13&sessionId=11&resId=0&materialId=slides&confId=6360`

[6] M. E. Peskin, "Estimation of LHC and ILC Capabilities for Precision Higgs Boson Coupling Measurements," arXiv:1312.4974 [hep-ph].

[7] T. Barklow, private communication.

[8] D. M. Asner, T. Barklow, C. Calancha, K. Fujii, N. Graf, H. E. Haber, A. Ishikawa and S. Kanemura *et al.*, "ILC Higgs White Paper," arXiv:1310.0763 [hep-ph].

[9] G. Wilson, "Investigating In-Situ $\sqrt{s}$ Determination with $\mu\mu(\gamma)$," ECFA LC2013, `http://agenda.linearcollider.org/getFile.py/access?contribId=140&sessionId=16&resId=1&materialId=slides&confId=5840`.

[10] H. Li, "Higgs Recoil Mass and Cross-Section Analysis at ILC AND Calibration of the CALICE SiW ECAL Prototype," PhD Thesis Université Paris Sud - Paris XI (2009), `http://tel.archives-ouvertes.fr/tel-00430432/fr/`

[11] M. S. Amjad, M. Boronat, T. Frisson, I. Garcia, R. Poschl, E. Ros, F. Richard and J. Rouene *et al.*, "A precise determination of top quark electro-weak couplings at the ILC operating at $\sqrt{s} = 500$ GeV," arXiv:1307.8102.

[12] F. Richard, "Present and future constraints on top EW couplings," arXiv:1403.2893 [hep-ph].

[13] J. Tian, "Study of Higgs self-coupling at the ILC based on full detector simulation at $\sqrt{s} = 500\,\mathrm{GeV}$ and $\sqrt{s} = 1\,\mathrm{TeV}$," April 2013, LC-REP-2013-003, `http://www-flc.desy.de/lcnotes/notes/LC-REP-2013-003.pdf`

[14] C. Dürig, private communication, PhD Thesis in preparation.

[15] S. Dawson *et al.*, "Higgs Working Group Report of the Snowmass 2013 Community Planning Study," arXiv:1310.8361 [hep-ex].

[16] S. Kanemura, E. Senaha, T. Shindou and T. Yamada, JHEP **1305** (2013) 066 [arXiv:1211.5883 [hep-ph]].

[17] T. Behnke, J. E. Brau, P. N. Burrows, J. Fuster, M. Peskin, M. Stanitzki, Y. Sugimoto and S. Yamada *et al.*, "The International Linear Collider Technical Design Report - Volume 4: Detectors," arXiv:1306.6329 [physics.ins-det].

[18] C. Adolphsen *et al.*, "The International Linear Collider Technical Design Report - Volume 3.II: Accelerator Baseline Design," arXiv:1306.6328 [physics.acc-ph].

[19] G. Moortgat-Pick *et al.*, Phys. Rept. **460** (2008) 131 [hep-ph/0507011].

[20] T. Abe *et al.* [ILD Concept Group - Linear Collider Collaboration], *The International Large Detector: Letter of Intent*, [arXiv:1006.3396 [hep-ex]].

[21] J. Tian, private communication.

[22] R. Yonamine *et al.*, Phys. Rev. D **84** (2011) 014033 [arXiv:1104.5132 [hep-ph]].

[23] A. Mustafayev and X. Tata, Indian J. Phys. **88** (2014) 991 [arXiv:1404.1386 [hep-ph]].

[24] M. Berggren, F. Brümmer, J. List, G. Moortgat-Pick, T. Robens, K. Rolbiecki and H. Sert, Eur. Phys. J. C **73** (2013) 2660 [arXiv:1307.3566 [hep-ph]].

[25] H. Baer, V. Barger, P. Huang, D. Mickelson, A. Mustafayev, W. Sreethawong and X. Tata, JHEP **1312** (2013) 013 [arXiv:1310.4858 [hep-ph], arXiv:1310.4858].

[26] S. Dittmaier *et al.* [LHC Higgs Cross Section Working Group Collaboration], arXiv:1101.0593 [hep-ph].

[27] T. Barklow, "Using the Hadronic Recoil Measurement in Higgs Coupling Fits", presentation at International Workshop on Future Linear Colliders, Belgrade, Serbia, October 6-10, 2014, `http://agenda.linearcollider.org/contributionDisplay.py?sessionId=0&contribId=137&confId=6389`